

The Hellenic Subduction System: High-Pressure Metamorphism, Exhumation, Normal Faulting, and Large-Scale Extension

Uwe Ring,^{1,*} Johannes Glodny,² Thomas Will,¹ and Stuart Thomson³

¹Lehrstuhl für Geodynamik, Universität Würzburg, 97074 Würzburg, Germany; email: uwe.ring@canterbury.ac.nz, thomas.will@uni-wuerzburg.de; ²Deutsches GeoForschungsZentrum, 14473 Potsdam, Germany; email: glodnyj@gfz-potsdam.de; ³Department of Geosciences, University of Arizona, Tucson, Arizona 85721; email: thomson@email.arizona.edu

Annu. Rev. Earth Planet. Sci. 2010. 38:45–76

First published online as a Review in Advance on January 4, 2010

The *Annual Review of Earth and Planetary Sciences* is online at earth.annualreviews.org

This article's doi:
10.1146/annurev.earth.050708.170910

Copyright © 2010 by Annual Reviews.
All rights reserved

0084-6597/10/0530-0045\$20.00

*On leave from Department of Geological Sciences, University of Canterbury, Christchurch 8140, New Zealand.

Key Words

extrusion wedge, metamorphic core complex, geochronology, tectonics, Aegean Sea, Greece

Abstract

The Cenozoic history of the retreating Hellenic subduction system in the eastern Mediterranean involves subduction, accretion, arc magmatism, exhumation, normal faulting, and large-scale continental extension from ~60 Mya until the Recent. Ages for high-pressure metamorphism in the central Aegean Sea region range from ~53 Ma in the north (the Cyclades islands) to ~25–20 Ma in the south (Crete). Younging of high-pressure metamorphism reflects the southward retreat of the Hellenic subduction zone. The shape of pressure-temperature-time paths of high-pressure rocks is remarkably similar across all tectonic units, suggesting a steady-state thermal profile of the subduction system and persistence of deformation and exhumation styles. The high-pressure metamorphic events were caused by the underthrusting of fragments of continental crust that were superimposed on slab retreat. Most of the exhumation of high-pressure units occurred in extrusion wedges during ongoing lithospheric convergence. At 23–19 Mya large-scale lithospheric extension commenced, causing metamorphic core complexes and the opening of the Aegean Sea basin. This extensional stage caused limited exhumation at the margins of the Aegean Sea but accomplished the major part of the exhumation of high-grade rocks that formed between 21 and 16 Mya in the central Aegean. The age pattern of extensional faults and contoured maps of fission-track cooling ages do not show a simple southward progression. Our review of lithologic, structural, metamorphic, and geochronologic data is consistent with a temporal link between the draping of the subducted slab over the 660-km discontinuity and the large-scale extension causing the opening of the Aegean Sea basin.

Ma: million years

Subduction: underthrusting of one plate below its neighbor at a convergent plate boundary

Slab: tabular body of subducted lithosphere in the mantle

IMPORTANCE OF SUBDUCTION PHENOMENA

On a global scale, $\sim 80\%$ of the consumption of plates occurs at subduction zones, which have a total length of $\sim 51,000$ km and an average subduction rate of 62 km per million years (62 km Ma^{-1}). Subduction zones are not fixed in position with respect to the overriding plate; some advance toward the overriding plate whereas others retreat (or roll back) seaward (Chase 1979, 1980; Uyeda 1982; Royden & Husson 2006). The latter situation commonly arises when the rate of the overriding plate's convergence with the trench is smaller than the subduction rate of the underthrusting plate (Dewey & Bird 1970, Royden 1993). This circumstance results in regional, commonly large-scale horizontal extension in the overriding plate (Figures 1–3) (Garfunkel et al. 1986, Lonergan & White 1997). Important parameters causing rollback of subduction zones appear to be (a) a slow-down of absolute plate motion relative to the lower mantle hot-spot reference frame (Elsasser 1971, Faccenna et al. 2003), (b) the negative buoyancy of the subducting slab (Royden 1993), and (c) an increase in slab length to ~ 150 km (Schellart 2005).

There is debate about whether the rollback of subduction zones is steady or nonsteady on timescales of Ma to tens of Ma. During incipient subduction the slab advances toward the overriding plate (Uyeda 1982). Because the negative buoyancy of the subducting slab primarily controls rollback, the latter will become important in the course of progressive subduction of heavy slabs (Royden 1993). Once these heavy slabs have been subducted to depths exceeding ~ 80 km and their lengths are $> \sim 150$ km, rollback may become important (Schellart 2005). Episodic rollback

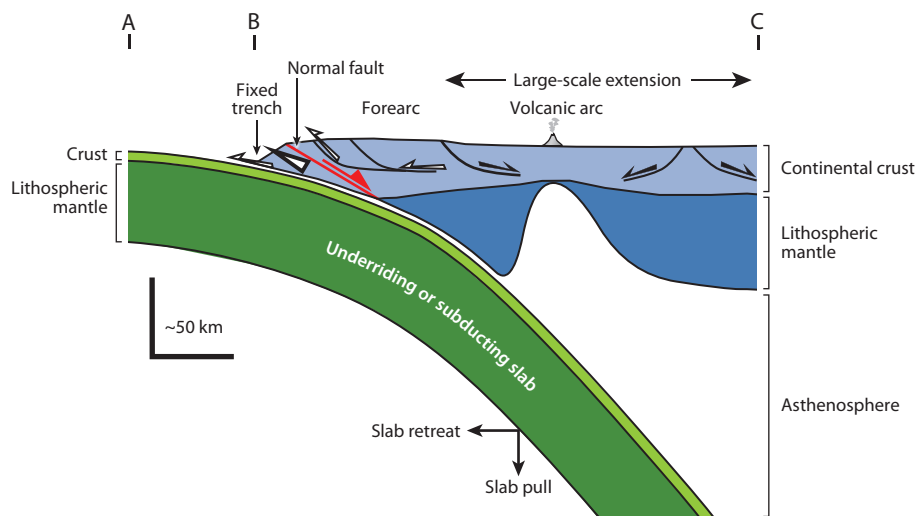


Figure 1

Simplified sketch showing retreating subduction zone defined by a subduction rate (vector AB) that is greater than the convergence rate (vector AC) (Royden 1993). The overriding plate with the trench above the retreating subduction zones must extend to compensate for the difference between the subduction and convergence rates. In the Aegean, large-scale extension of the overriding plate presently occurs in front of and behind the volcanic arc. During retreat or rollback, the mantle flow field includes flow along the strike of the trench induced by slab rollback and classical corner flow produced by the convergence velocity (Long & Silver 2008). Note also that extrusion wedges at the leading edge of the overriding plate form above the retreating subduction zones (the top of the extrusion wedge is marked by the red normal fault).

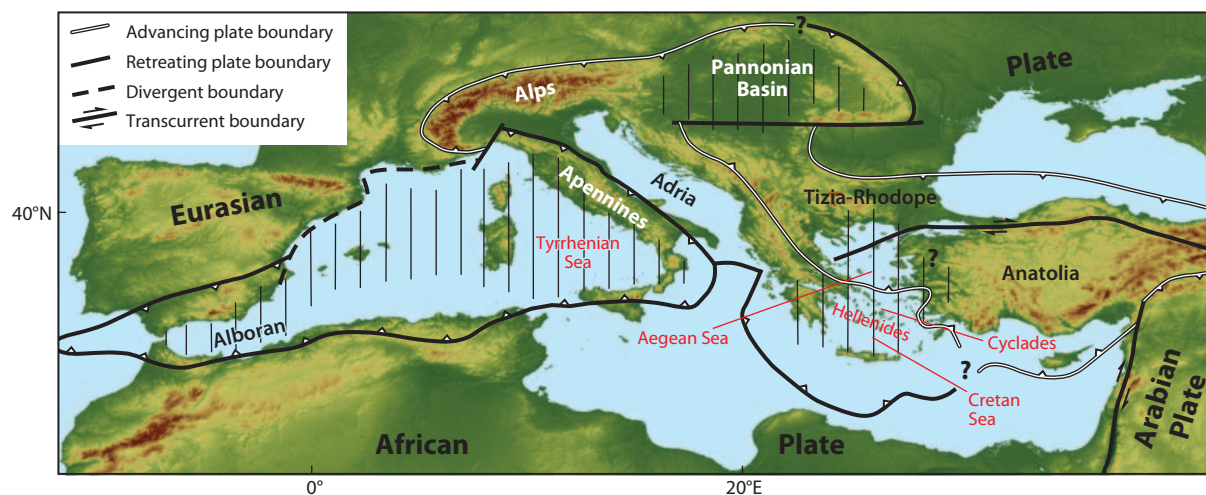


Figure 2

Highly simplified tectonic map of the Mediterranean plate-boundary zone showing retreating, advancing, and major transcurrent plate boundaries (*barbs on overriding plate*). The three major plates (Eurasian, African, and Arabian) are shown, and the microplates between them are shown schematically. These microplates are currently forming (e.g., Anatolia) or have been amalgamated to Eurasia in the past (e.g., Adria). Vertical lines indicate highly extended regions above retreating plate boundaries. The Hellenides, the Aegean and Cretan Seas, and the Cyclades are shown.

might result from the interaction of the subducting slab with the upper/lower mantle discontinuity at 660-km depth (see 660-km Discontinuity sidebar), which tends to slow down slab descent into the lower mantle (Ringwood 1991, Funicello et al. 2003). It also might result from the arrival of fragments of buoyant continental lithosphere in the subduction zone (Brun & Faccenna 2008). Isacks & Molnar (1969) showed that the slab-pull force of the subducting slab increases to a maximum when the slab tip approaches the 660-km discontinuity. When the slab first starts to interact with this discontinuity, it folds (Figure 3). The seaward migration of the retreating slab relative to the trench accelerates considerably when the slab drapes over the 660-km discontinuity (Schellart 2005). At this stage, much of the overriding plate experiences a major pulse of horizontal extension (Figure 3).

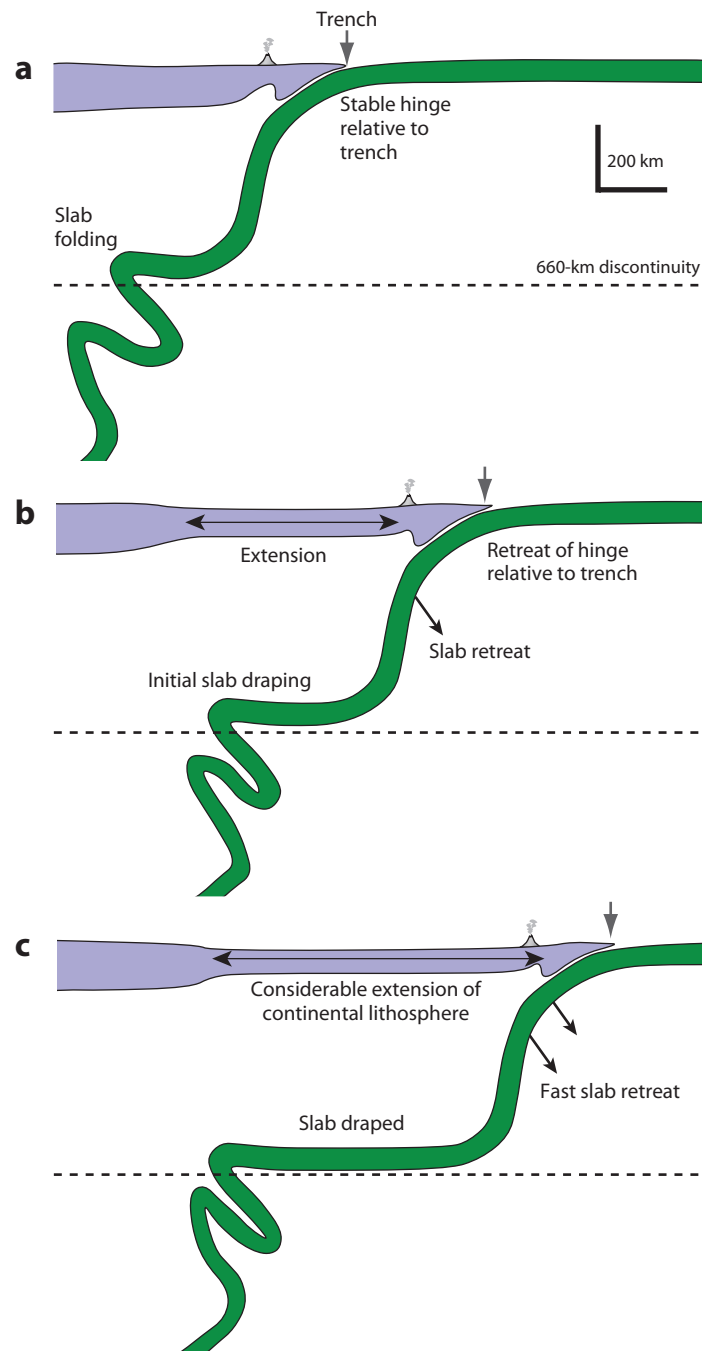
Much of the discussion about the rollback of subducting slabs is driven by numerical modeling. The assumptions and simplifications of these models for subduction-zone rollback far outstrip observations and data collected in the field, but nature is invariably more complex than numerical and scaled analog material models can simulate. We therefore set out to review data collected in the field and in the laboratory on lithologic characteristics, as well as deformation, metamorphic evolution, and geochronologic signatures of the Hellenic subduction system in the eastern

Slab draping: process by which hindering of slab descent into the lower mantle causes the slab to drape over the 660-km discontinuity

660-km DISCONTINUITY

The 660-km discontinuity is an important boundary that separates the upper and lower mantle. This boundary is defined by a phase change from spinel to perovskite and a related marked increase in density. This and the buoyancy associated with the discontinuity slow down the penetration of the subducting slab into the lower mantle.

Mediterranean to infer tectonic processes in a retreating subduction zone. The Hellenic subduction system is a well-studied example of a retreating subduction zone (**Figure 2**). It has a fairly limited trench-parallel length (~600–800 km). Such laterally narrow subduction zones typically have rapid retreat rates and form concave profiles (Schellart 2005).



THE HELLENIC SUBDUCTION ZONE AND AEGEAN GEOLOGY

Geology of the Hellenides

The Hellenides form an arcuate orogen above the subducting Hellenic slab. Customarily, the geology of the Hellenides is subdivided into several tectonic domains (**Figure 4**) characterized by rock type, stratigraphy, tectonometamorphic history, and preorogenic paleogeography (Robertson et al. 1991). In the Hellenides of the Aegean transect, these are, from north to south, (a) the Srednogie Block and Rhodope-Sakarya Block, (b) the Vardar-Izmir Oceanic Unit, (c) the Pelagonian-Lycian Block, (d) the Pindos Oceanic Unit (including the Cycladic Blueschist Unit), (e) the Tripolitza Block, (f) the Ionian Block, and (g) the East Mediterranean Ocean (Dürr et al. 1978, Bonneau 1984, Jacobshagen 1986, van Hinsbergen et al. 2005).

The Srednogie, Rhodope, and Sakarya continental fragments were amalgamated with Eurasia between ~185 and >100 Mya (Mposkos & Kostopoulos 2001, Krohe & Mposkos 2002). The Vardar-Izmir Oceanic Unit was subducted beneath the Srednogie and Rhodope-Sakarya blocks (**Figure 5**) during the Cretaceous (~145–65 Mya). The Vardar-Izmir Oceanic Unit includes mainly Jurassic (~200–145 Mya) ophiolitic rocks, which are representative of a suprasubduction zone environment. A volcanic arc related to the subduction of the Vardar-Izmir Oceanic Unit was initiated in southern Bulgaria at ~90–75 Mya (von Quadt et al. 2005) (**Figures 4** and **5**).

The Pelagonian-Lycian Block occurs structurally below the Vardar-Izmir Oceanic Unit. Parts of the Vardar-Izmir Oceanic Unit and parts of the Pelagonian-Lycian Block were metamorphosed under blueschist-facies conditions between ~125 and 85 Mya (Lips et al. 1999, Sherlock et al. 1999, Ring & Layer 2003). Above the southern edge of the Pelagonian-Lycian Block, the Meso-Hellenic and Thrace troughs formed as forearc basins at the beginning of the Eocene (~56–50 Mya) (Vamvaka et al. 2006, Huvaz et al. 2007).

The units to the south—i.e., in the footwall of the Pelagonian-Lycian Block—do not have a Cretaceous orogenic history. They became involved in subduction orogenesis and associated high-P metamorphism at least 20 Ma later than the Pelagonian-Lycian Block and the Vardar-Izmir Oceanic Unit.

The Pindos Oceanic Unit is a heterogeneous paleogeographic domain that involves oceanic crust and continental basement-cover sequences. These different units are part of an accretionary complex that formed between ~55 and 30 Mya. In the Cyclades, the uppermost part of the Pindos Oceanic Unit is the highly attenuated ophiolitic Selçuk Mélange (Okrusch & Bröcker 1990), which now traces the suture between the Pindos Oceanic Unit and the overlying Pelagonian-Lycian Block (Ring & Layer 2003). Slivers of oceanic crust (gabbro, plagiogranite, basalt) that formed at ~80–65 Mya (Keay 1998, Tomaschek et al. 2003) are incorporated in the ophiolitic

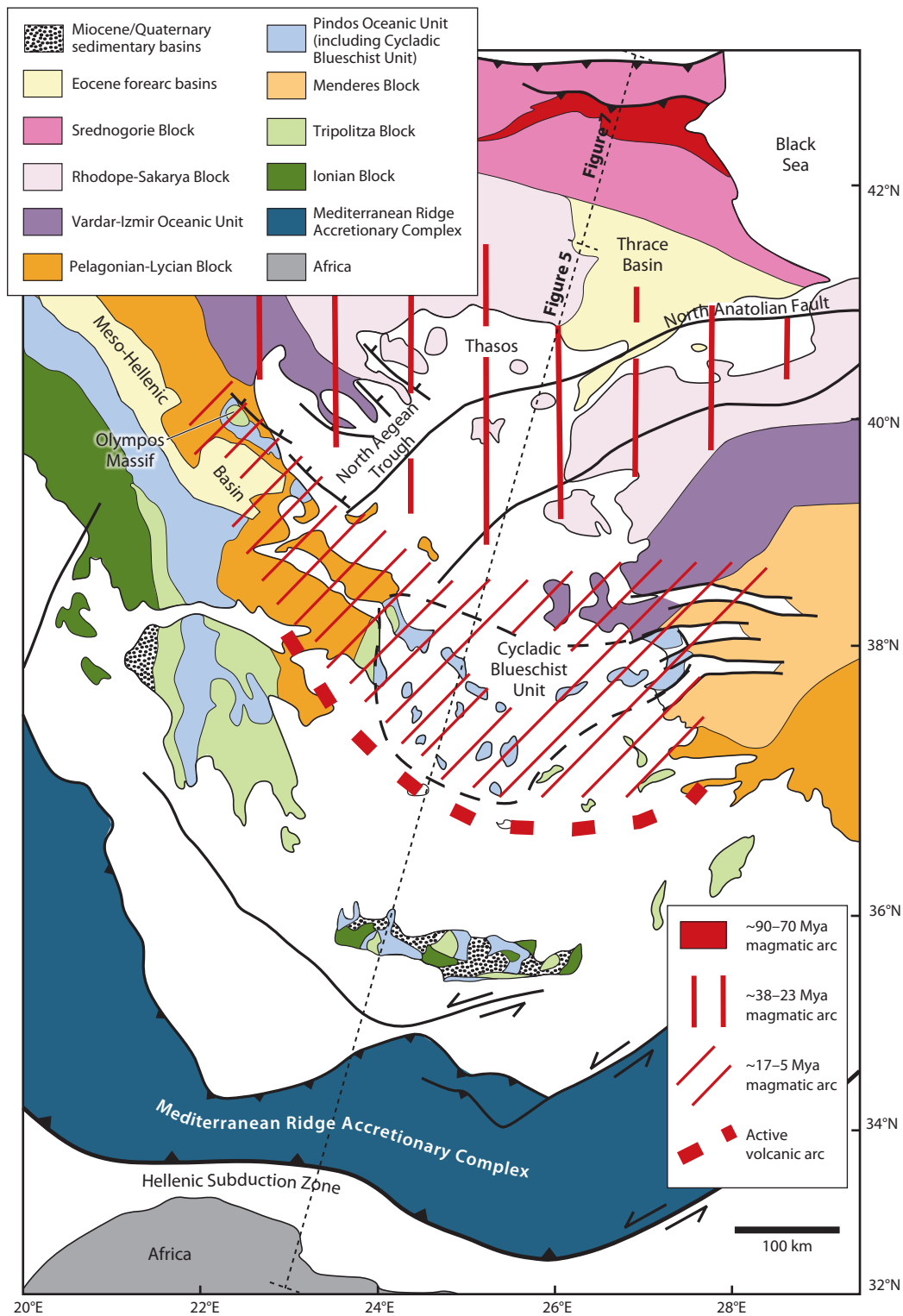
Block: a continental fragment or microplate

Oceanic unit: a tectonic entity that includes oceanic crust

Mya: millions of years ago

Figure 3

Interaction of a subducting slab with the 660-km discontinuity (modified from Schellart 2005). (a) Subducting slab penetrates 660-km discontinuity. When the slab starts to interact with the discontinuity, it folds; at this stage, the subducting hinge is stable relative to the overriding plate with the trench. For the hinge to stay stable or even advance, the slab must fold again and penetrate the discontinuity. (b) The slab starts to drape over the 660-km discontinuity, possibly controlled by a slow-down in the subduction rate. The draping of the slab onto the discontinuity allows the slab to maintain a self-similar geometry, and for geometric reasons, the draping must result in pronounced retreat and a major phase of horizontal extension in the overriding plate. The rate of retreat is somewhat limited by the length of the slab parallel to the trench. Rapid slab retreat is more likely to occur with short slabs (600–800 km in length), such as the Hellenic slab. (c) Advanced stage of slab draping associated with fast hinge retreat and the accompanying large-scale extension of the overriding plate.



Selçuk Mélange. Below the Selçuk Mélange, the continental rocks of the Cycladic Blueschist Unit constitute the most deeply exhumed parts of the Hellenides. The Cycladic Blueschist Unit comprises a Carboniferous (~360–300 Mya) basement of schist and orthogneiss, and a late Carboniferous to post-Carboniferous passive-margin sequence of marble, metapelite, and volcanics (Dürr et al. 1978, Ring & Layer 2003). The passive-margin sequence is unconformably overlain in southwestern Turkey by mid-Paleocene to late Paleocene flysch (~62–56 Mya) (Özer et al. 2001). Initial flysch deposition slightly predates the beginning of sedimentation in the Meso-Hellenic and Thrace forearc basins. The flysch and forearc-basin sediments were deposited in response to the inception of subduction of the Pindos Oceanic Unit.

The Tripolitza Block represents a continental platform unit of Triassic to Eocene age (~250–40 Mya) and is partly overlain by late Eocene to early Oligocene flysch (~35–25 Mya) (Jacobshagen 1986). Underthrusting of the Tripolitza Block commenced at ~35–30 Mya (Thomson et al. 1998a, Sotiropoulos et al. 2003). In the Cyclades, high-P rocks of the Tripolitza Block are locally exposed in tectonic windows through the overlying Cycladic Blueschist Unit (Godfriaux 1968, Shaked et al. 2000, Ring et al. 2001). Farther south in the Peloponnese and in Crete, the rocks of the Tripolitza Block and the Pindos Oceanic Unit are only weakly metamorphosed. Here, the Cretan detachment tectonically separates the Tripolitza Block from underlying high-P rocks of the Ionian Block that are ~25–20 Ma old (Fassoulas et al. 1994, Jolivet et al. 1996, Thomson et al. 1999). The Ionian Block comprises late Carboniferous to possibly Triassic (~310–220 Mya) rocks overlain by limestone and late Eocene to Miocene flysch (~35–10 Mya) (Jacobshagen 1986).

The southernmost and most outboard tectonic domain of the Hellenides is the Mediterranean Ridge Accretionary Complex (**Figure 4**; also see Kopf et al. 2003). The onset of accretion occurred at ~19 Mya during ongoing subduction of Triassic (~250–200 Mya) oceanic crust of the East Mediterranean Ocean (van Hinsbergen et al. 2005). Along the central Mediterranean Ridge, this oceanic crust of the East Mediterranean Ocean has been completely consumed, and the leading edge of the African passive continental margin is currently entering the subduction zone.

How Many Subduction Zones?

The geology of the Aegean Sea region provides evidence for at least three oceanic domains (the Vardar-Izmir Oceanic Unit, Pindos Oceanic Unit, and East Mediterranean Ocean) and intervening isolated continental fragments (**Figure 6**). There is debate about whether all those domains were subducted and accreted along a single subduction zone (Spakman et al. 1993, Robertson et al. 1996, Ricou et al. 1998, Faccenna et al. 2003, van Hinsbergen et al. 2005). Two general ways to resolve this problem have been applied: geologic reconstructions and interpretation of tomographic images. Each of these is discussed below.

Figure 4

Simplified tectonic map of the Aegean region showing the main tectonic zones above the Hellenic subduction zone (modified from Jolivet & Brun 2010). The Mediterranean Ridge represents the modern accretionary wedge that is bounded to the north by a major backthrust system. Also shown are the Meso-Hellenic and Thrace forearc basins, which formed at ~56–50 millions of years ago (Mya) (Vamvaka et al. 2006, Huvaz et al. 2007) and were later, at least in part, thrust to more southerly positions. Red-line patterns indicate the positions of subduction-related magmatic-arc rocks from ~38 Mya to the Recent, according to Fytikas et al. (1984), Barr et al. (1999), and Pe-Piper & Piper (2002). The migration of this magmatic arc in the overriding plate mimics the retreat of the Hellenic slab. Also shown in the north (*red*) is a volcanic arc related to the subduction of the Vardar-Izmir Oceanic Unit at ~90 Mya (von Quadt et al. 2005). The dashed black line indicates the position of the cross sections shown in **Figures 5** and **7**. The North Anatolian Fault reached the Sea of Marmara no earlier than ~0.2 Mya (Şengör et al. 2005).

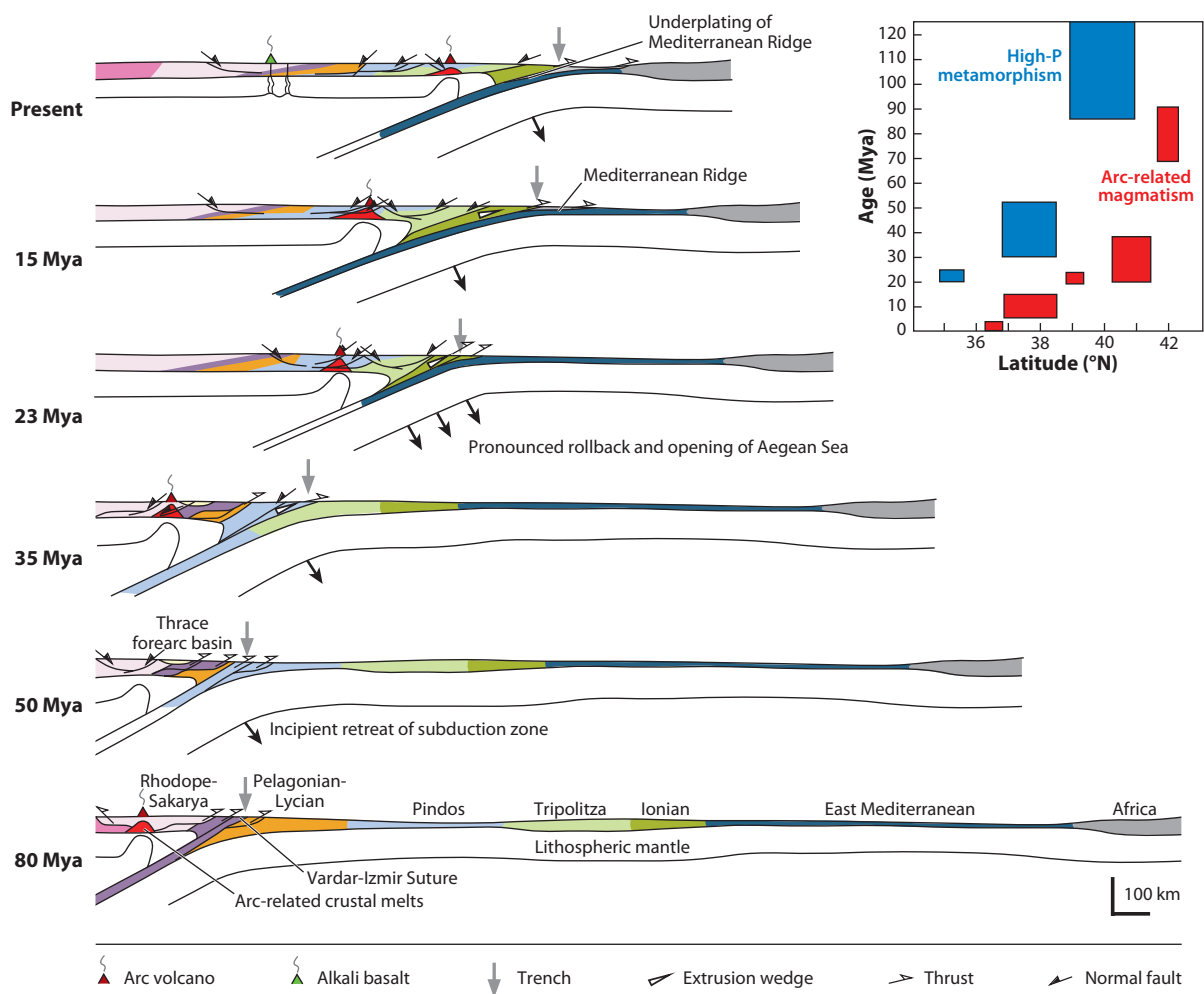


Figure 5

Interpretative cross sections showing the development of the subduction system from ~80 Mya to the present. At ~80 Mya the system was contractional and high-P metamorphism occurred in the Vardar-Izmir Oceanic Unit and the Pelagonian-Lycian Block. At ~50 Mya subduction of the Pindos Oceanic Unit caused reactivation of the Pelagonian-Lycian Block and extensional deformation in the Rhodope-Sakarya Block. At this stage, after ~5–10 Ma of subduction of the Pindos Oceanic Unit, the system changed from an advancing/stationary subduction zone to a retreating subduction zone. Hardly any magmatic arc was developed at this time. At ~35 Mya the Tripolitza Block entered the subduction zone and a mature magmatic arc developed in northern Greece. High-P rocks of the Cycladic Blueschist Unit were exhuming in extrusion wedges above the subduction zone. At ~23 Mya a major Aegean-wide extensional event started, and important low-angle extensional faults formed across the entire Aegean Sea. The trench moved considerably outboard. At ~15 Mya the magmatic arc of the retreating subduction system was in the Cyclades; Aegean-wide extensional faulting continued. Presently the leading edge of the African Plate is entering the convergence zone; the North Anatolian Fault is propagating into the North Aegean region, causing rift-related alkaline and subalkaline volcanism. The inset on the upper right shows an age versus latitude diagram of arc-related magmatism (red) and subduction-related high-P metamorphism (blue) (adapted from Faccenna et al. 2003). The diagram shows a time gap in subduction-related activity between ~75 and 55 Mya.

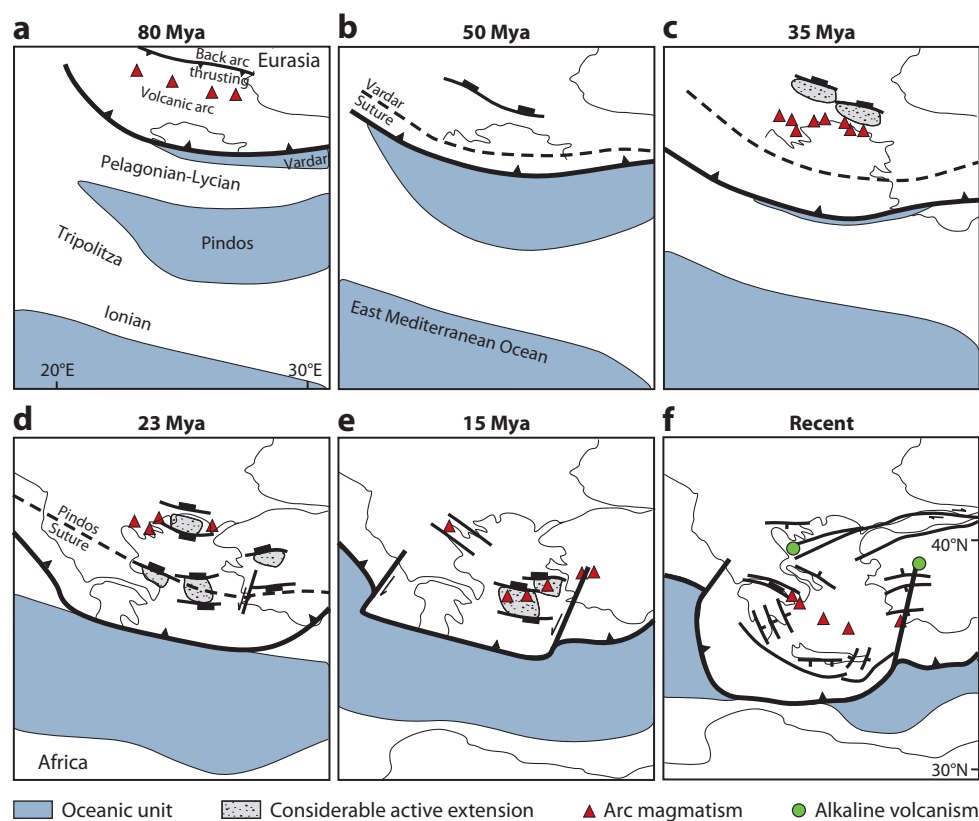


Figure 6

Tectonic reconstruction of subduction in the eastern Mediterranean since ~80 Mya relative to fixed Eurasia (modified from Brun & Faccenna 2008) (compare with **Figure 5**). (a) Final closure of the Vardar-Izmir Oceanic Unit and arc magmatism (red triangles) in southern Bulgaria. (b, c) Stages of progressive closure of the Pindos Oceanic Unit and mature stage of arc volcanism at ~35 Mya. (d) Incipient subduction of the East Mediterranean Ocean and initiation of a phase of fast rollback and associated lithospheric extension in the overriding plate. (e) The subduction system in the Aegean Sea region moved considerably outboard owing to rollback of this segment of the slab. This spatially restricted slab rollback increased the curvature of the Hellenic margin and possibly caused tears (de Boorder et al. 1998) on both sides of the retreating slab. (f) Present situation with propagation of the North Anatolian Fault into the northern Aegean and associated alkaline volcanism (green circles). Alkaline volcanism also occurs in western Turkey.

1. The geologic reconstructions are largely based on the recognition of magmatic arcs, forearc basins, subduction-related flysch deposition, and the age of subduction-related high-P metamorphism. Jurassic and Cretaceous northward subduction occurred along the Vardar-Izmir Suture and created the volcanic arc in southern Bulgaria at ~90–75 Mya (**Figures 5 and 6**). Because the initial subduction of the Pindos Oceanic Unit took place after a distinct time gap of ≥ 20 Ma, Ricou et al. (1998) considered that the subduction of the Pindos Oceanic Unit resulted from the formation of a new Cenozoic subduction zone. The inception of Cenozoic subduction at ~60 Mya marks a distinct southward shift of the subduction system across the Pelagonian-Lycian Block and a southward shift of the magmatic arc by > 100 km (**Figure 6**; also see Ricou et al. 1998, Pe-Piper & Piper 2002, Marchev et al. 2004). The ophiolitic Selçuk

Slab tear: a near-vertical crack in the slab that forms in response to differential motion of adjacent parts of the slab

Mélange of the Pindos Oceanic Unit would be the suture between units that were already amalgamated to Eurasia in the Cretaceous (Srednogorie, Rhodope-Sakarya, Vardar-Izmir, and Pelagonian-Lycian) and the incoming units farther south (Pindos, Tripolitza, Ionian, and East Mediterranean). The magmatic arc related to the inception of Cenozoic subduction formed in the latest Eocene, approximately 38–35 Mya, in the northern Aegean Sea region in the Rhodope-Sakarya Block (Fytikas et al. 1984, Pe-Piper & Piper 2002). The remnants of oceanic crust in the ophiolitic Selçuk Mélange that are ~80–65 Ma old (see above) set a maximum age for subduction and suturing of the Pindos Oceanic Unit.

2. The interpretation of tomographic images used to resolve the one-or-more-subduction-zones debate is inherently speculative because of those images' limited resolution. In the Aegean, tomography shows a broad high-velocity anomaly in the upper mantle and one in the mantle just below the 660-km discontinuity (Spakman et al. 1993, Bijwaard et al. 1998) (**Figure 7**). Directly above the 660-km discontinuity the slab is thicker than in its upper part; this thickening of the high-velocity anomaly seems to result from folding (Faccenna et al. 2003). The tomographic image further shows that the slab is horizontal above the 660-km discontinuity over a length of ~300 km (van Hinsbergen et al. 2005). The anomaly in the lower mantle is ~800 km long but approximately twice as thick as the upper-mantle slab (**Figure 7**, inset).

An important question is whether the upper- and lower-mantle anomalies are directly connected and thus whether they reflect subduction of one and the same slab. Faccenna et al. (2003) and van Hinsbergen et al. (2005) interpreted the tomographic images to represent continuous subduction of a single slab, possibly since ~200 Mya. Both groups agree that the lower-mantle anomaly represents ~1100–1500 km of material subducted in the Mesozoic. The upper-mantle anomaly represents at least 1000 km of subduction in the Cenozoic (~65 Mya to the present) (Faccenna et al. 2003; **Figure 7**). In this view, the Cenozoic subduction zone would comprise the subduction and partial accretion of the Pindos Oceanic Unit at ~60 Mya, of the Tripolitza and Ionian Blocks, and of the East Mediterranean Ocean. Cenozoic subduction followed Mesozoic subduction after the gap in subduction activity of at least 20 Ma. In other words, there was possibly continuous convergence with a ≥ 20 -Ma halt in documented subduction processes between the Mesozoic and Cenozoic.

A tear in the slab below western Turkey has been suggested by de Boorder et al. (1998) and is thought to have caused (sub)alkaline, in part shoshonitic, magmatism. When this tear formed is not exactly clear.

In summary, the interpretation of Faccenna et al. (2003) and van Hinsbergen et al. (2005) of continuous subduction since ~200 Mya is commonly accepted among Aegean tectonicians. However, a two-subduction-zone scenario as envisaged by Ricou et al. (1998) cannot fully be ruled out if the two subducting slabs are stacked one on top of the other beyond the resolution of the tomographic imaging. Whether there is one subducting slab or two (a Mesozoic one and a Cenozoic one), it seems evident that the subducting slab(s) apparently interacted differently with the 660-km discontinuity through time. In the Jurassic and Cretaceous periods, the subducting slab penetrated through the 660-km discontinuity and the subduction system did not roll back to any significant degree. At ~85 Mya, after the Pelagonian-Lycian Block was amalgamated to Eurasia, there was a time gap of ≥ 20 Ma before the Pindos Oceanic Unit started to subduct at ~60 Mya. If more than 1000 km of subduction occurred since ~60 Mya, the tomographic data shown in **Figure 7** would suggest that the Cenozoic portion of the subducting slab represents the upper-mantle high-velocity anomaly and that it was draped over the 660-km discontinuity over a length of ~300 km (van Hinsbergen et al. 2005).

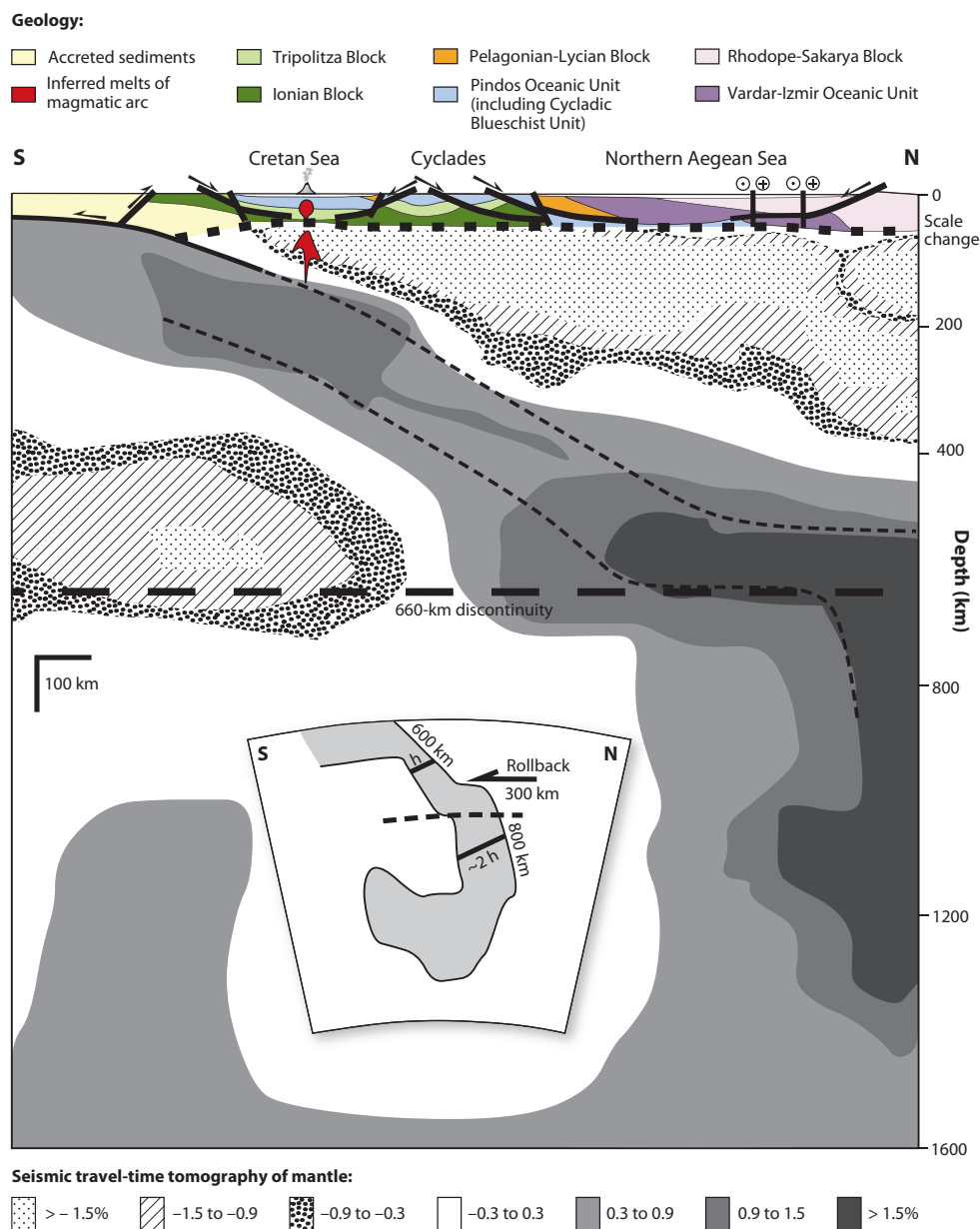


Figure 7

Generalized crustal N-S cross section through the Aegean Sea showing the shortening structure of the Mediterranean Ridge Accretionary Complex and major low-angle normal and dextral strike-slip faults to the north of it. The dotted line marks the crust-mantle boundary. A northward-dipping Wadati-Benioff plane can be followed down to a depth of 180 km (Hatzfeld 1994, Papazachos & Nolet 1997). A tomographic image for the Aegean mantle shows a high-velocity anomaly of the descending slab down to ~1800 km (Spakman et al. 1993, Bijwaard et al. 1998). The geometry of the high-velocity anomaly changes distinctly across the 660-km discontinuity (see inset; also see van Hinsbergen et al. 2005). The dashed lines represent our interpretation of the Cenozoic portion of the downgoing slab, whose backward draping over the 660-km discontinuity was documented by van Hinsbergen et al. (2005). The Aegean extensional region is underlain by a low-velocity upper mantle. The crustal part of the cross section is vertically exaggerated by a factor of two.

Cenozoic Rollback of the Slab

There is no evidence for slab rollback in the Jurassic and Cretaceous (Faccenna et al. 2003), and apparently the subduction system advanced to the north (in present-day coordinates relative to a fixed Eurasia) or remained stationary during those times. Rollback of the Hellenic slab, however, is well established after ~ 55 – 50 Mya and is recorded by (a) the southward migration of the magmatic arc into the former forearc and accretionary wedge, (b) the distinct southward shift of the age of subduction-related high-P metamorphism, and (c) a slow-down in the rate of plate convergence. Each of these is discussed below.

Southward migration of the magmatic arc into the former forearc and accretionary wedge.

Several researchers have reported evidence that rollback of the Hellenic slab became important during the Eocene (~ 55 – 35 Mya) (Thomson et al. 1998a, Faccenna et al. 2003, Kounov et al. 2004), as indicated by a distinct southward migration of the magmatic arc (Fytikas et al. 1984, Pe-Piper & Piper 2002, Marchev et al. 2004) (Figures 5 and 6). Arc-related magmatic rocks in the northernmost Aegean date back to ~ 38 to 35 Mya (Pe-Piper & Piper 2002, Marchev et al. 2004, Kounov et al. 2004). [There are earlier granite intrusions between ~ 52 – 42 Mya (Ovtcharova et al. 2003), but they are apparently not related to a magmatic arc.] Robust U-Pb ages from zircons of exposed arc-related granodioritic and monzogranitic plutons in the Cyclades range from ~ 17 to 11 Mya (Henjes-Kunst et al. 1988; Keay 1998; Keay et al. 2001; Brichau et al. 2007, 2008; Bolhar et al. 2010), and ages of volcanic rocks range from 12 to 5 Mya (Fytikas et al. 1984). This indicates that the magmatic arc reached the Cyclades at ~ 17 Mya. The arc shifted south to its present position at ~ 4 – 3 Mya. The age data on subduction-related volcanic rocks suggest that this retreat occurred at a crude rate of ~ 20 km Ma^{-1} since ~ 38 Mya (Fytikas et al. 1984).

Distinct southward shift of the age of subduction-related high-pressure metamorphism.

The earliest recorded high-P metamorphism in the Cycladic Blueschist Unit occurred at ~ 53 Mya at a depth of ~ 50 – 60 km (see review of metamorphic and geochronologic data below). A Paleocene subduction rate of 30 km Ma^{-1} (Faccenna et al. 2003) and a slab dip of 30 – 40° (Schellart 2005) suggest that the related subduction episode commenced at ~ 60 Mya. The latter age would broadly be in line with the onset of flysch sedimentation in the Cycladic Blueschist Unit (Özer et al. 2001) and also in line with the slightly delayed initiation of forearc sedimentation in the Rhodope-Sakarya Block to the north (Vamvaka et al. 2006, Huvaz et al. 2007). Kounov et al. (2004), Bonev et al. (2006), and Bonev & Beccaletto (2007) showed that extensional deformation in the Rhodope-Sakarya Block in southern Bulgaria commenced at 55 Mya, at approximately the same time that high-P metamorphism occurred in the Cycladic Blueschist Unit. Overall, the data suggest that subduction-zone retreat in the northern Aegean started at ~ 55 Mya and caused extension in northern Greece and Bulgaria.

Slow-down in the rate of plate convergence. Dewey et al. (1989) and Rosenbaum et al. (2002) showed that the relative plate motion between Africa and Eurasia came almost to a halt between ~ 65 and 52 Mya. It is almost inescapable to conclude that at this stage the rate of subduction was greater than the convergence rate, which would have promoted slab rollback.

METAMORPHISM


High-Pressure Metamorphism in the Hellenic Subduction Zone

Most units in the Aegean were involved in the Cenozoic subduction-accretion system and they record high-P metamorphism. This metamorphism ranges from low-grade high-P (e.g., Crete)

to eclogite facies (in most parts of the Cycladic Blueschist Unit). In **Figure 8** we have compiled conventional pressure and temperature (P-T) data and P-T path segments that were inferred from phase-diagram modeling. In contrast to conventional geothermobarometry, the phase-diagram approach is commonly better suited for evaluating the P-T evolution of metamorphic rocks (see **Supplemental Material** for details about phase-diagram modeling; follow the **Supplemental Materials link** from the Annual Reviews home page at <http://www.annualreviews.org>).

Figure 8 demonstrates that the inferred P-T paths all document pronounced cooling during decompression. Overall, the P-T-path data obtained for the blueschist and greenschist units of the central and southern Aegean strongly imply that the thermal conditions above the Cenozoic Hellenic subduction zone remained fairly stable through time during the southward migration of the subduction system. The shape and direction of the inferred P-T paths from islands in the northern Cyclades (Tinos, Samos), from islands in the central (Syros) and southern Cyclades (Sifnos, Amorgos), and from Crete are strikingly similar and indicate coeval decompression and cooling (**Figure 8**). Tectonically the same result emerges: The inferred P-T paths for various tectonic subunits of the Cycladic Blueschist Unit—i.e., the ophiolitic Selçuk Mélange on Tinos and Syros, as well as the cover (Sifnos) and the basement (Samos) of the continental basement-cover sequence—are similar to P-T paths from the high-P units of the Tripolitza and Ionian rocks on Amorgos and Crete (**Figure 8**). Below we provide a review of critical isotopic age data for distinct metamorphic P-T stages.

P-T: pressure and temperature

 **Supplemental Material**

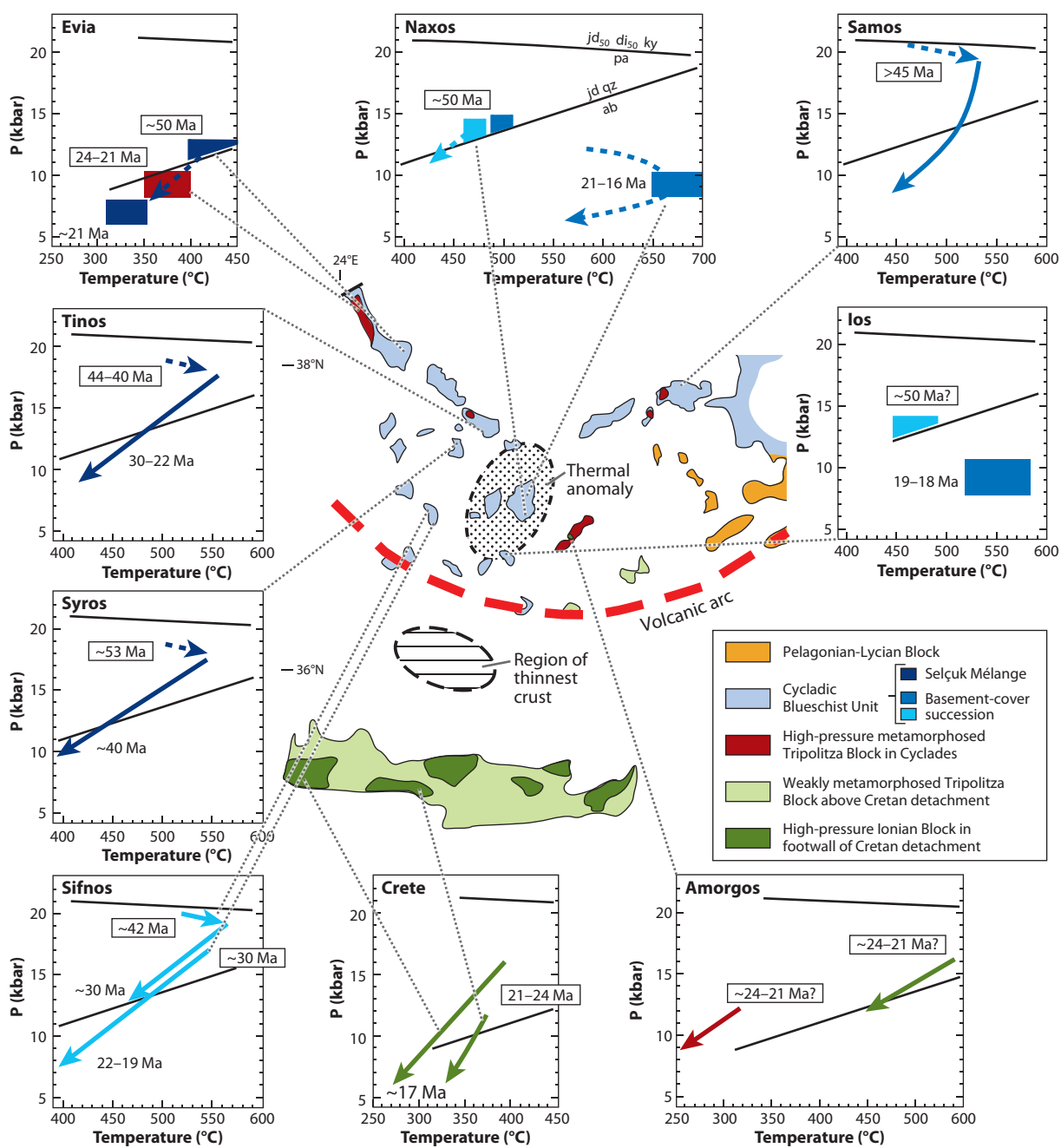
After the High-Pressure Metamorphic Events

It has been previously thought that the P-T evolution in the central Aegean involved an Eocene (50–40 Mya) high-P event followed by isothermal decompression and a subsequent distinct early Miocene (25–20 Mya) greenschist- to amphibolite-facies stage (see review in Okrusch & Bröcker 1990). As already pointed out by Schmädicke & Will (2003), the shape of the inferred P-T paths is not compatible with isothermal decompression and an extension-driven exhumation mechanism. In a number of cases, deformation-induced mineral reactions produced greenschist-facies mineral assemblages. These occur, for instance, in parts of the thrust units on Sifnos Island relatively soon (less than ~5–10 Ma) after the two high-P stages at 42–40 Mya and ≥ 30 Mya. On other islands, greenschist-facies mineral equilibration was intimately associated with extensional deformation that started in Tinos at ~22 Mya but not until ~10 Ma later on Ikaria and Serifos (see below for geochronologic details). Field observations show that greenschist-facies overprints are typically localized along broad shear zones, which acted as fluid pathways. The greenschist-facies overprints also involve hydration reactions. We therefore propose that these deformation-related metamorphic equilibration stages were controlled by the local availability of fluids and do not reflect regional P-T “controlled” metamorphic events.

A distinct early Miocene high-temperature metamorphic event occurred on the islands of Naxos and Paros where migmatites formed (Jansen 1973, Jansen & Schuiling 1976). Buick & Holland (1989) showed that this amphibolite- to granulite-facies metamorphism occurred during and probably as a consequence of extensional deformation. P-T conditions reached 8–10 kbar at 650–700°C (Buick & Holland 1989). For southern Naxos, Avigad (1998) demonstrated that there was cooling after the preceding Eocene high-P event (> 12 kbar, 400–480°C), which indicates that the thermal pulse in the Miocene was associated with a pronounced temperature increase of up to ~300°C.

Because most of the Aegean is submerged, the regional extent of the Naxos/Paros thermal anomaly is not well known. Thomson et al. (2009) showed that metamorphic temperatures on Ios

Island to the south of Naxos reached $\geq 500\text{--}550^\circ\text{C}$ and ~ 9 kbar in the early Miocene (**Figure 8**). The temperatures for the Eocene high-P event on Ios were distinctly lower than those reached during the early Miocene temperature-dominated metamorphism. This, together with structural data, indicates that Ios is located on the southern margin of the thermal anomaly, which forms a distinct feature in the central Aegean (**Figure 8**).



Annu. Rev. Earth Planet. Sci. 2010.38:45-76. Downloaded from www.annualreviews.org. Access provided by University of Oregon on 01/14/18. For personal use only.

The metamorphic pressures for the high-P events (Ios: 12–13 kbar, Grütter 1993; Naxos: >12 kbar, Avigad 1998) and high-T events (Naxos and Ios: ~9 kbar) show a difference of ~3–4 kbar. This indicates only moderate exhumation of ~15 km between the two events and points to more pronounced exhumation of ~30 km after the early Miocene high-T event within the Naxos/Paros-Ios thermal anomaly area.

TIMING AND EVOLUTION OF DEFORMATION AND METAMORPHISM

Age Constraints: High-Pressure Metamorphism and Early Exhumation

In many places, the high-P metamorphic assemblages are well preserved, and subsequent, exhumation-related changes in P-T did not leave any imprint in the rocks. Elsewhere, high-P rocks are partially retrogressed to lower-P blueschist- or greenschist-facies assemblages. Only locally are the rocks fully transformed to low-P assemblages, allowing isotopic dating of exhumation-related overprints. Typically, the completely retrogressed rocks are spatially related to shear zones or zones of fluid infiltration, which indicates that free aqueous fluids played a key role in metamorphic reequilibration (e.g., Bröcker et al. 1993). This implies that isotopic data for greenschist-facies assemblages may not directly date the time when the rocks were subjected to greenschist-facies P-T conditions but may instead date the time of fluid-facilitated mineral reactions. Thus, the earliest greenschist-facies age recorded for a high-P unit may be the best approximation to the true age of exhumation to low-P greenschist-facies conditions. In the following, we review some of the existing age data from north to south and for the various units of the Hellenic subduction-accretion system (also see **Supplemental Material**; follow the **Supplemental Materials link** from the Annual Reviews home page at <http://www.annualreviews.org>).

The Pelagonian-Lycian Block records blueschist-facies conditions in the Cretaceous. The exact timing is poorly constrained to ~125–85 Mya (Schermer et al. 1990, Lips et al. 1999). An exhumation-related tectonic reactivation starting at blueschist- to greenschist-facies conditions at ~61–54 Mya and ceasing at greenschist-facies conditions at ~45 Mya (Schermer et al. 1990, Lips et al. 1999) is important for the Cenozoic evolution of Hellenic slab subduction.

High-P metamorphism in the underlying Cycladic Blueschist Unit is directly related to Cenozoic slab subduction. Published ages for high-P metamorphism and for exhumation stages show

Pressure and depth: for continental crust (average density ~2800 kg m⁻³), metamorphic P increases by 1 kbar with every 3.5 km of depth


 **Supplemental Material**

Figure 8

Summary of P-T data from the central Aegean and Crete, with age information. Numbers in rectangles refer to high-P stage; other numbers refer to exhumation-related greenschist- to amphibolite-facies overprints, or for Crete, cooling through the closure temperature of fission tracks in zircon. The P-T data from the Cycladic Blueschist Unit have been subdivided into the ophiolitic Selçuk Mélange and the tectonically underlying basement-cover succession. P-T data sources: Evia: Katzir et al. (2000), Shaked et al. (2000); Samos: Will et al. (1998); Naxos: Buick & Holland (1989), Avigad (1998); Ios: Grütter (1993), Thomson et al. (2009); Sifnos: Schmädicke & Will (2003); Amorgos: Rosenbaum et al. (2007); Crete: Jolivet et al. (1996), Thomson et al. (1999). Geochronologic data from Seidel et al. (1982), Wijbrans & McDougall (1988), Henjes-Kunst et al. (1988), Bröcker et al. (1993), Lister & Raouzaos (1996), Jolivet et al. (1996), Thomson et al. (1999), Keay et al. (2001), Brix et al. (2002), Ring & Layer (2003), Forster & Lister (2005), Duchêne et al. (2006), Ring et al. (2007a,b), and J. Glodny (unpublished data). The black lines in the graphs represent the reactions jadeite (jd) + quartz (qz) → albite (ab) (*bottom lines*), and jadeite (jd₅₀) + diopside (di₅₀) + kyanite (ky) → paragonite (pa) (*top lines*). Note the occurrence of Tripolitza rocks in windows in the Cycladic Blueschist Unit and the thermal anomaly in the center of the Aegean. Kincaid & Griffiths (2003) showed that the following events occur during rollback: Subduction flow is driven around and beneath the sinking plate, and velocities increase within the mantle wedge and are focused toward the center of the plate. Therefore the overriding plate heats more along the centerline, which may explain the thermal anomaly in the Naxos/Paros-Ios region.

some regional variation. On Evia, incipient high-P metamorphism started at ~50 Mya (Maluski et al. 1981) (**Figure 8**). High-P conditions of the Cycladic Blueschist Unit persisted there until ~33 Mya, when the rocks started to be exhumed and finally reequilibrated under greenschist-facies conditions at ~21 Mya (Ring & Layer 2003, Ring et al. 2007a). For the Cyclades islands, recent data indicate that the Cycladic Blueschist Unit may be internally structured, consisting of different tectonometamorphic slices (cf. Forster & Lister 2005). For example, high-P rocks of northern Syros provide strong evidence for early high-P metamorphism at ~53 Mya, based on U-Pb zircon and Ar-Ar phengite data (Tomaschek et al. 2003, Putlitz et al. 2005). The earliest greenschist-facies overprint on Syros is dated at ~40 Mya (our own unpublished Rb-Sr mineral data). A similar situation appears in Samos in the eastern Aegean. Here, high-P metamorphism took place before 45 Mya (Ring & Layer 2003). Incipient exhumation of high-P rocks started at ~42 Mya under high-P conditions and proceeded under greenschist-facies conditions until ~32 Mya (Ring et al. 2007b). In contrast, in northern Sifnos in the southwest Cyclades, earliest high-P metamorphism occurred at ~42 Mya, followed by blueschist- to greenschist-facies retrogression at ~30 Mya (Altherr et al. 1979, Wijbrans et al. 1990, Lister & Raouzaïos 1996, Forster & Lister 2005; our own unpublished data). The age pattern for northern Sifnos is similar to that described for the Cycladic Blueschist Unit on Tinos: high-P metamorphism at 44–40 Mya, with early blueschist- to greenschist-facies overprints near 30 Mya (Bröcker et al. 1993). The southern part of Sifnos is home to yet another high-P unit (Schmädicke & Will 2003), located structurally below the ~42-Ma old high-P complex of northern Sifnos. It records a high-P overprint at ≥ 30 Mya and greenschist-facies reworking at ~22–19 Mya (Altherr et al. 1979, Wijbrans et al. 1990; our own unpublished data) (**Figure 8**).

From this data set it appears that for each high-P slice, significant time elapsed (between 5 and 15 Ma) before it was exhumed enough to facilitate decompression-related mineral reactions. Combined structural and geochronologic data from Sifnos indicate that high-P and exhumation ages decrease toward lower structural position of slices within the Cycladic Blueschist Unit. Younging of both high-P and exhumation ages progressed toward deeper tectonic slices—i.e., from the ophiolitic Selçuk Mélange to the underlying basement-cover sequence of the Cycladic Blueschist Unit. The structurally downward younging trend in general coincides with a younging trend of the subduction system and the magmatic arc toward the south. However, this geographic trend is less clear in some areas because high-P metamorphism on Syros appears to be earlier than on Tinos, which is located north of Syros. We hypothesize that the original geometric pattern of age distributions has been distorted by Miocene to Recent large-scale extension (see below) and block rotations (Duermeijer et al. 2000, van Hinsbergen et al. 2006).

Rocks of the Tripolitza Block structurally below the Cycladic Blueschist Unit are present in several tectonic windows in the Cyclades (on Evia, Samos, Amorgos, and Tinos; **Figure 8**). In the windows of the Cycladic realm, the Tripolitza Block records high-P metamorphism of 8–10 kbar and 350–400°C (Shaked et al. 2000), and age data for high-P metamorphism fall consistently between ~24 and 21 Mya (Ring et al. 2001, Ring & Reischmann 2002, Ring & Layer 2003).

The southernmost and structurally lowest exposed belt of high-P rocks above the Hellenic subduction system is the Ionian Block in parts of Crete and the Peloponnese. This unit experienced blueschist-facies metamorphism (350–400°C, ~10–16 kbar) at ~25–20 Mya (Seidel et al. 1982, Jolivet et al. 1996) and cooled through ~240–280°C at ~17 Mya (Thomson et al. 1998a). This Miocene age confirms Crete as one of the youngest blueschist-facies belts in the world.

The present crustal thickness of western Crete is ~40–50 km; the bottom ~20 km of this crust are interpreted to comprise newly accreted sediments (Knapmeyer & Harjes 2000, Meier et al. 2007). This indicates that high-P rocks are currently forming beneath Crete.

Age Constraints: Extension and Detachment Faulting in the Aegean

Extensional deformation was established by 23–19 Mya. Extension is evident from the formation of both steep normal faults and, more importantly, activity of large-scale low-angle extensional detachments. It appears that there is no clear regional trend in the isotopic ages for extension. Instead, extension began between 23 and 19 Mya all over the region. In the northern Aegean, age constraints come from the Thasos detachment, activated at 23–21 Mya (Wawrzenitz & Krohe 1998), and from the Symvolon shear zone/Strymon valley detachment system in northern Greece, which was initiated near 22 Mya (Dinter 1998). Farther south, low-angle extensional faults have been active since ~23 Mya on the flanks of the Olympos Massif (**Figure 4**; also see Schermer et al. 1990). In the Cyclades, both north- and south-dipping extensional detachment zones exist, giving way to the formation of the Naxos/Paros metamorphic core complex. Initiation of extensional deformation on Naxos is constrained to ≥ 20.7 Mya, based on U-Pb data for zircon that formed in extension-induced melts (Keay et al. 2001). On Samos, the oldest record of extensional fault movement is ~20–18 Ma in age (Kumerics et al. 2005). Further south in Ios, extension along the South Cyclades shear zone and the associated Ios detachment commenced at ~19 Mya (Thomson et al. 2009) and controlled the opening of the Cretan Sea basin.

In **Figures 9** and **10** we show contoured maps for apatite fission-track (AFT) and zircon fission-track (ZFT) cooling ages, respectively (also see Fission-Track Cooling Ages sidebar, below). The maps show similar overall age patterns. For apatite, with a closure temperature of ~110°C (Reiners & Brandon 2006), the contouring reveals old ages (>20 Ma) in western Turkey, the islands of Donoussa and Amorgos in the east-central Aegean, and Crete. For the latter islands the old AFT ages are all from the hanging walls of detachment faults and thus provide a maximum age for the detachment fault. The youngest AFT ages (<8 Ma) occur on Ikaria, Mykonos, Naxos, and Serifos (largely coinciding with the thermal anomaly) in the footwalls of major detachments in the central Aegean. For zircon, with a closure temperature of 240–280°C (Reiners & Brandon 2006), the regional distribution of cooling ages is similar; Crete is an exception in that it shows a distinct westward-younging age pattern. The older ZFT ages in eastern Crete are only a few Ma younger than the peak of high-P metamorphism. The pattern of ZFT ages from the footwall of the Cretan detachment suggests that there may be more than one detachment horizon, with an “older” Cretan detachment in the east. The supposedly “younger” Cretan detachment in the west coincides with distinctly higher elevations and thicker crust in western Crete than in eastern Crete (Knapmeyer & Harjes 2000). Alternatively, the Cretan detachment could root at much deeper levels in the west than in the east. Indeed, maximum metamorphic pressures in the footwall rocks of the Cretan detachment are ~6 kbar higher in western Crete than in eastern Crete (Jolivet et al. 1996).

An area in the eastern Cyclades, eastern Crete, and western Turkey cooled through the fission-track closure temperatures fairly quickly between ~ 30 and 20 Mya. Cooling ages to the west are younger. The fission-track contour maps show that there is no simple north-to-south propagation in the younging of ZFT and AFT ages that would mimic the southward retreat of the Hellenic subduction zone or the gradual southward migration of the magmatic arc. Therefore it appears that other processes controlled cooling and exhumation in the brittle crust. The

Detachment: large-scale, low-angle normal fault typically tens of km² or more in area that separates a hanging-wall block from its footwall block

AFT: apatite fission-track

ZFT: zircon fission-track

FISSION-TRACK COOLING AGES

The closure temperature, T_c , for fission tracks is a function of the activation energy for diffusion, a proportionality constant, and the cooling rate. For apatite T_c is ~110°C; for natural, radiation-damaged zircon T_c is 240–280°C. Thus both systems track cooling in the brittle crust.

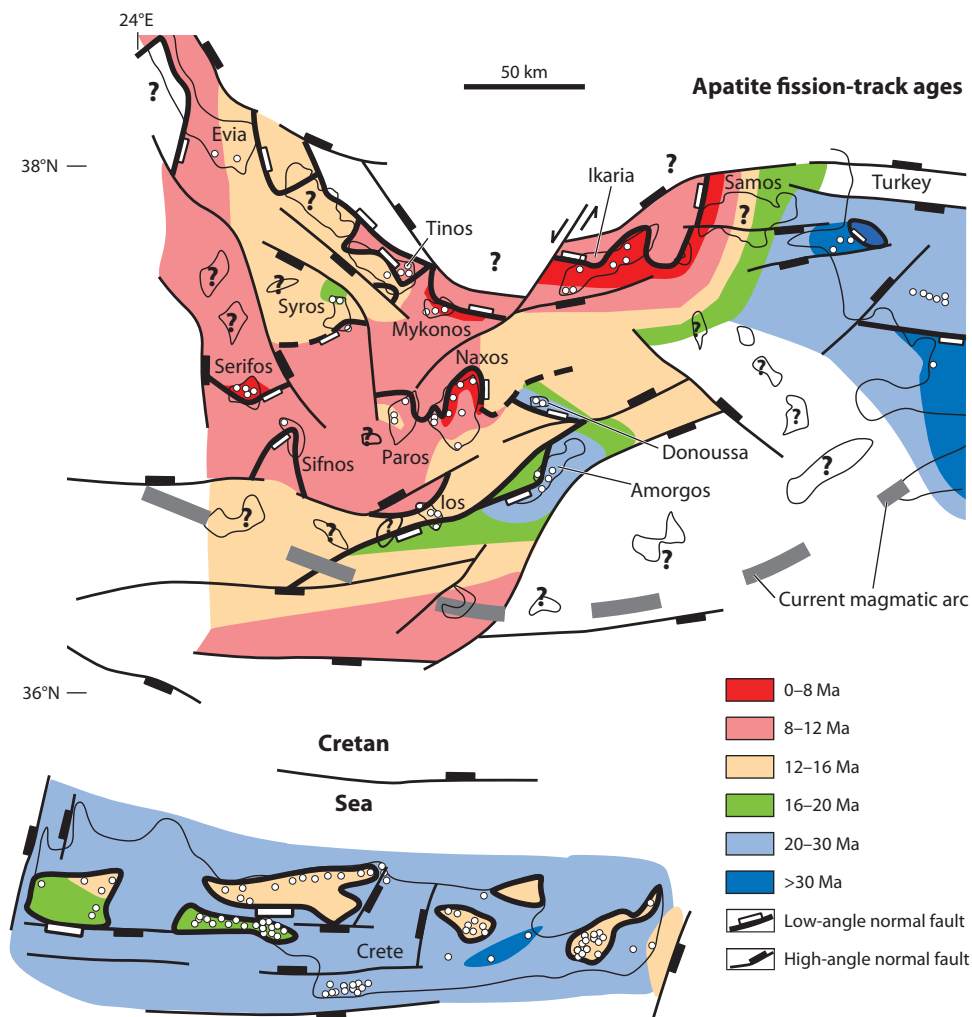


Figure 9

Contouring of 249 apatite fission-track (AFT) ages from the central Aegean, western Turkey, and Crete. The contouring reveals old ages (>20 Ma) in western Turkey, on the islands of Donoussa and Amorgos, and in rocks above the Cretan detachment on Crete. The youngest AFT ages (<8 Ma) occur on islands that are almost adjacent to the islands with old ages, e.g., on Icaria and Naxos next to the westernmost Turkey/Donoussa area. The white sample dots indicate areas from which we have data, and question marks indicate islands from which no data exist. Data are from Thomson et al. (1998a,b; 1999; 2009), Brix et al. (2002), Hejl et al. (2002), Ring et al. (2003; 2007a,b; 2009), Kumerics et al. (2005), Brichau et al. (2006, 2007, 2008, 2010), and S. Thomson (unpublished data). A full sample list can be obtained from S. Thomson.

fission-track age patterns mainly reflect fluctuations in the regional partitioning of extensional deformation and related exhumation from 23 Mya to the Recent.

The area of old fission-track ages in the east extends across the southward-shifting magmatic arcs, indicating that the heat flux associated with arc magmatism had no major influence on tectonically controlled upper-crustal cooling (Brichau et al. 2006). It seems that cooling, at least in the brittle crust, was controlled by the rapidly exhuming footwall blocks of extensional detachments.

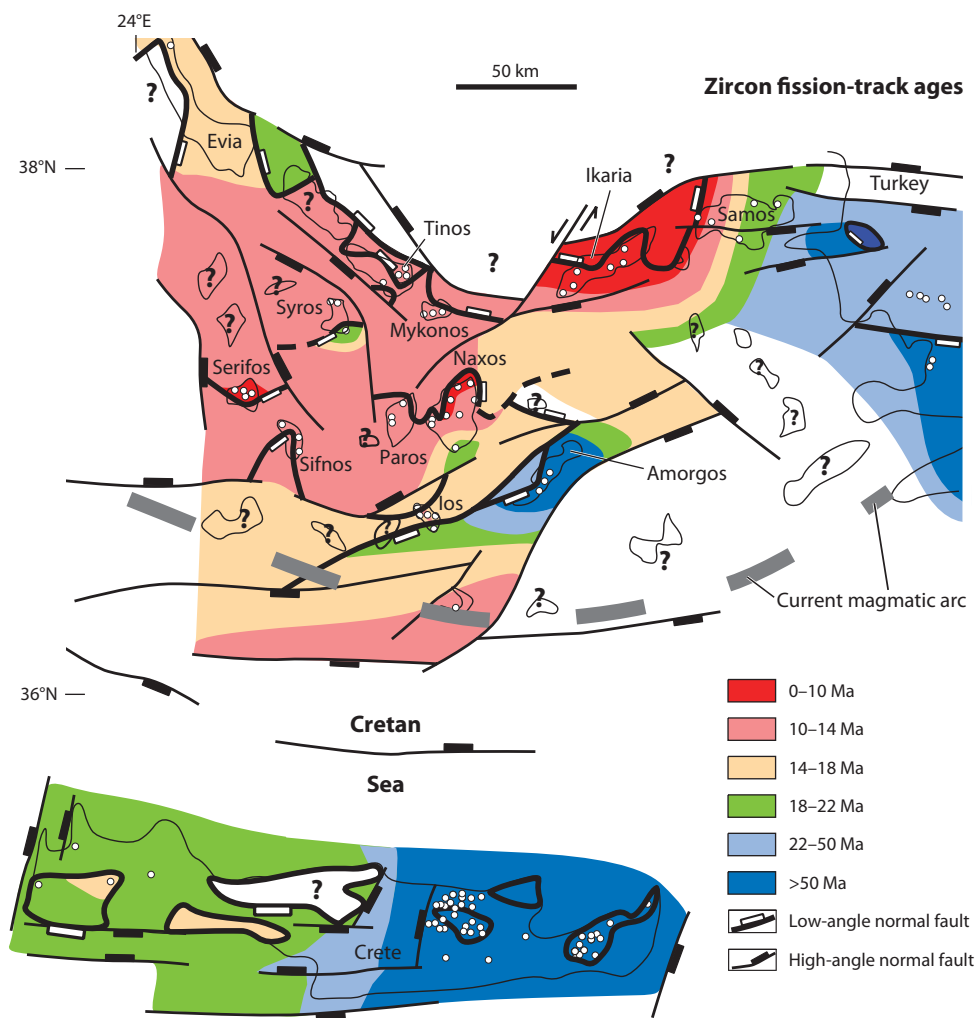


Figure 10

Contouring of 167 zircon fission-track (ZFT) ages from the central Aegean, western Turkey, and Crete. The trends are fairly similar to those of the AFT ages. A surprising and not well-understood feature is the east-to-west younging of ZFT ages on Crete. We have no ZFT ages for Donoussa, but ages must be older than the AFT ages of ~25 Ma. Data are from Thomson et al. (1998a,b; 1999; 2009), Brix et al. (2002), Hejl et al. (2002), Ring et al. (2003; 2007a,b; 2009), Kumerics et al. (2005), Brichau et al. (2006, 2007, 2008, 2010), and S. Thomson (unpublished data).

EXHUMATION OF HIGH-PRESSURE ROCKS IN AND ABOVE THE HELLENIC SUBDUCTION ZONE

In the following we use the terms shortening-related normal fault and extension-related normal fault for distinguishing normal faults at the top of extrusion wedges that formed during lithospheric shortening from those that formed during later lithospheric extension (cf. Ring & Glodny 2010). These differences are important for distinguishing whether exhumation of high-P rocks occurred

during overall horizontal shortening in extrusion wedges in a suprasubduction zone setting, or during wholesale horizontal lithospheric extension in the overriding plate at a stage when the trench had moved farther outboard. The bulk of the exhumation of high-P rocks, at least toward a mid-crustal position, typically occurs relatively soon ($< \sim 15$ Ma) after these rocks formed as a consequence of lithospheric convergence and deep underthrusting (Avigad et al. 1997; Reddy et al. 1999; de Sigoyer et al. 2004; Glodny et al. 2005; Ring et al. 2007a,b). Extrusion wedges are the ideal tectonic setting for structurally achieving this exhumation.

Aegean Extrusion Wedges

Recent studies at the western and eastern edges of the Aegean, in Evia as well as Samos and adjacent western Turkey (Ring et al. 2007a,b), showed that extrusion wedges formed in the Eocene at ~ 42 – 32 Mya (Samos/western Turkey) and early Oligocene at ~ 33 – 21 Mya (Evia). Both extrusion-wedge systems were active for ~ 10 Ma (see Extrusion Wedges sidebar, below). The recognition of these two extrusion wedges solved the long-standing problem of how the early preextension exhumation of the Cycladic Blueschist Unit was structurally accomplished. P-T estimates in conjunction with isotopic age dating of deformation in the bounding shear zones demonstrated 30–40 km of late Eocene exhumation of the Cycladic Blueschist Unit in Samos and western Turkey. The extrusion wedge on Evia accomplished ~ 8 – 15 km of syn-subduction exhumation.

Thomson et al. (1999) and Doutsos et al. (2000) described an early Miocene extrusion wedge from Crete that was active for ~ 6 – 8 Ma and accomplished most of the exhumation of the Cretan high-P rocks from > 30 km. In the Cycladic and Cretan cases, normal faulting at the top of the extruding wedges was not associated with the development of extensional graben in their hanging walls. This indicates that the normal faults did not result from regional horizontal extension, and that they are therefore shortening-related normal faults.

Extrusion wedges have so far not been reported from elsewhere in the Cycladic Blueschist Unit and the blocks to the south. Trotet et al. (2001) speculated that Eocene extrusion wedges had formed on Sifnos and Syros, but they provide no critical age information demonstrating coeval motion on a basal thrust and a shortening-related normal fault at the top. Ring & Layer (2003) discussed whether the putative extrusion wedge on Sifnos formed in the early Oligocene; however, unambiguous evidence for the Sifnos extrusion wedge is lacking.

EXTRUSION WEDGES

An extrusion wedge is a fault-bounded slice that may form where plates converge in a subduction zone. It is defined by a basal thrust that allows one plate to slip beneath another and a normal-sense shear zone or fault at its top. The two shear zones or faults allow the wedge to extrude laterally and upward between the converging plates. Thus, the normal-sense shearing at the top of the wedge is not an effect of regional extension because the region is undergoing overall horizontal shortening. To prove the existence of an extrusion wedge, it is critical to demonstrate that the basal thrust and the normal fault at the top moved simultaneously. Because the basal thrust and the normal fault at the top of an extrusion wedge operate in concert during overall horizontal shortening, considerable tectonic exhumation of the extruding wedge does not cause substantial attenuation of the crust. It is crucial to define the distribution of internal deformation in an extrusion wedge. If deformation is concentrated along the boundaries, it results in the extrusion of a rigid crustal wedge. Alternatively, the deformation may be distributed throughout the wedge, resulting in ductile extrusion.

The reported cases of extrusion-wedge formation (Thomson et al. 1999; Doutsos et al. 2000; Ring et al. 2007a,b) showed that the wedges commonly achieved more than 50% of the exhumation of high-P rocks in or above the subduction channel. In the two examples from Evia and Samos/western Turkey, the normal fault at the top of the extrusion wedges developed in the ophiolitic Selçuk Mélange, which represents an ancient subduction thrust. As the subduction trench retreated, this former subduction thrust was reactivated as a shortening-related normal fault. Ring & Reischmann (2002) proposed a similar scenario for the Cretan detachment, highlighting the intimate relationship between extrusion wedges, pronounced tectonic exhumation, and the subduction system.

Large-Scale Extensional Deformation

Research over the past two decades has demonstrated the importance of Miocene low-angle ($<30^\circ$) extensional faults in the Aegean (Lister et al. 1984, Meulenkamp et al. 1988, Gautier et al. 1990, Avigad & Garfunkel 1991, Lee & Lister 1992, Krohe & Mposkos 2002). These extensional detachments accommodated the opening of the Aegean Sea triggered by the retreat of the Hellenic subduction zone (Buick 1991, Royden 1993). Faccenna et al. (2003) used a NNE-SSW balanced crustal section to calculate ~ 320 km of Cenozoic extension parallel to the subduction vector in the most highly stretched part of the Aegean.

The onset of large-scale extension in the Aegean most probably occurred no earlier than the early Miocene, as indicated by Aquitanian/Burdigalian (23–16 Mya) sediments in the oldest Aegean extensional basins (Büttner & Kowalczyk 1978, Böger 1983, Gautier et al. 1990, Sánchez-Gómez et al. 2002, Kuhlemann et al. 2004) and isotopic ages of extension-related mylonites starting at 23–19 Mya. Early Miocene extensional faults are well documented, for instance, on Tinos (Avigad & Garfunkel 1991), Naxos (Buick 1991), and in the northern Aegean (Wawrzenitz & Krohe 1998, Dinter 1998). It is likely that ages older than 23 Ma date shortening-related normal faulting at the top of extrusion wedges. Ring et al. (2007a) demonstrated this for Evia, where normal faulting at 33–21 Mya is associated with coeval thrusting structurally below the normal fault. Thus, normal faulting was not necessarily associated with regional horizontal lithospheric extension. Extension-related normal faults developed not before ~ 21 Mya on Evia (Ring et al. 2007a). Numerous studies have shown that most of the extensional detachments in the central Aegean experienced a significant phase of movement between ~ 17 and 8 Mya and facilitated emplacement of arc plutons (Buick 1991, Lee & Lister 1992, Kumerics et al. 2005, Brichau et al. 2008).

A widely held view is that large-scale Miocene-to-Recent extension occurred entirely in a back-arc setting (Lister et al. 1984, Gautier et al. 1990, Buick 1991, Faccenna et al. 2003). Nonetheless, several lines of evidence suggest that the inception of this extensional phase occurred before the magmatic arc was established:

1. Probably the least ambiguous example showing the relationship of large-scale extension to the migrating magmatic arc is the Cretan Sea basin, which is underlain by the most highly thinned part of the Aegean crust (**Figure 8**; ~ 15 – 16 km; also see Makris & Stobbe 1984). The Cretan Sea started to open at ~ 19 – 18 Mya, and the thinnest part of the basin is in front of the volcanic arc (**Figure 8**).
2. The ~ 22 -Ma old Tinos detachment was pierced by the arc-related Tinos monzogranite (Avigad & Garfunkel 1991) at 14 Mya (Brichau et al. 2007). The Naxos and Serifos arc-related granodiorites, as well as leucogranites on Ios, intruded into already operating extensional shear zones (Buick 1991; John & Howard 1995; Grasemann & Petrakakis 2007; Brichau et al. 2010; Thomson et al. 2009).

3. Fytikas et al. (1984) showed that the volcanic arc shifted southward and reached the Cyclades not before ~ 17 Mya. Large-scale extensional deformation, however, started at 23–19 Mya.
4. Robust U-Pb zircon ages from arc-related granites all span a narrow age range from 17 to 11 Mya (Henjes-Kunst et al. 1988; Keay 1998; Keay et al. 2001; Brichau et al. 2007, 2008; Bolhar et al. 2010). The plutons are 2–12 Ma younger than the inception of extensional faulting. The relation of the extensional faults and plutonism indicates that the intrusions were triggered by extension and not vice versa (Buick & Holland 1989; Brichau et al. 2006, 2007; Grasemann & Petrakakis 2007).

P-T work in exposed mylonitic shear zones (e.g., Tinos detachment) reveals that large-scale extensional shearing at 23–19 Mya commenced under (upper) greenschist-facies conditions and that the footwalls of the detachment reached the brittle crust soon afterward. However, in some parts of the Aegean extensional region, shearing commenced significantly later at 13–11 Mya (e.g., Ikaria; Kumerics et al. 2005).

The islands of Naxos and Paros in the central Cyclades are exceptions because metamorphism at ~ 21 –16 Mya reached upper amphibolite- to granulite-facies conditions (**Figure 8**). Buick & Holland (1989), Buick (1991), and Vanderhaeghe et al. (2007) argued that high-grade metamorphism and migmatization occurred during and probably as a consequence of extensional deformation. Thus, the high-T conditions may not be related to a regional-scale metamorphic event but instead to localized extensional deformation at ~ 21 Mya (Naxos) and ~ 19 –18 Mya (Ios).

The majority of the currently exposed extensional faults operated during the magmatic-arc stage between 17 and 8 Mya. After ~ 8 Mya, activity on the exposed low-angle extensional detachments ceased, and limited extension was—and still is, at least in Amorgos and Crete—restricted to high-angle faults. The high-angle normal faults in the current exposure level could be related to low-angle extensional faults in deeper parts of the crust. Interestingly, the rocks on Amorgos and Crete cooled through the fission-track closure temperatures early, but they record seismically active extensional faulting, again showing that the extensional structures conform to no distinct pattern or regional age trend.

Large-Scale Extension and Exhumation

Because of the low-angle geometry, each single large-displacement extensional detachment can readily accommodate a large amount of extension but only limited exhumation (Ring et al. 2003). Avigad et al. (1997) pointed out that most of the exhumation of the Cycladic Blueschist Unit occurred before the onset of back-arc extension. This finding has been corroborated by a number of recent quantitative studies on Evia, Tinos, Mykonos, Ikaria, Samos, Sifnos, Syros, and Serifos (Schmädicke & Will 2003; Kumerics et al. 2005; Brichau et al. 2007, 2008, 2010; Ring et al. 2003, 2007a,b), all of which have demonstrated that less than 15–25% of exhumation occurred in the footwalls of major extensional detachments.

Extension/exhumation relationships were distinctly different within the early Miocene thermal anomaly in the central Cyclades (**Figure 8**). As discussed above, ~ 30 km of exhumation of granulite-facies migmatitic rocks in Naxos was accomplished by extensional deformation from ~ 21 to 8 Mya (John & Howard 1995, Keay et al. 2001, Brichau et al. 2006, Seward et al. 2009). On Ios, the pressure conditions at the onset of extensional deformation were similar to those on Naxos and thus indicate the same amount of exhumation (Thomson et al. 2009). It follows that Miocene extensional deformation had a much more pronounced effect on exhumation in the central Aegean and caused the thermal anomaly there. The thermal anomaly occurs in the center of the Aegean extensional province, directly north of the area where the crust in the Cretan Sea is thinnest (**Figure 8**).

POSSIBLE SUBDUCTION, EXHUMATION, AND EXTENSION HISTORY

Continued Underthrusting

The subduction history of the Hellenic slab is one of continuous deep underthrusting over sustained periods of time (Faccenna et al. 2003, Ring & Layer 2003, van Hinsbergen et al. 2005). As shown by Wijbrans & McDougall (1988), Faccenna et al. (2003), Ring & Layer (2003), and van Hinsbergen et al. (2005), fragments of (thinned) continental crust were successively subducted, “peeled off” from the underlying lithosphere, and underplated; these fragments experienced high-P metamorphism in the subduction zone. Delamination of crustal slices has permitted the continuation of subduction of the mantle lithosphere since ~200 Mya (Thomson et al. 1999, Faccenna et al. 2003, van Hinsbergen et al. 2005).

The interpretation of the tomographic data argues for a fairly simple subduction of the slab from ~200 Mya until ~125–85 Mya (ages of high-P metamorphism in the Vardar-Izmir Oceanic Unit and the Pelagonian-Lycian Block). This phase of subduction involved the Srednogorie and Rhodope-Sakarya blocks, the Vardar-Izmir Oceanic Unit, and the Pelagonian-Lycian Block. Apparently the slab reached the 660-km discontinuity and penetrated it; the slab is now discernable in a lower-mantle high-velocity anomaly.

After the consumption and partial accretion of the Vardar-Izmir Oceanic Unit and the accretion of the Pelagonian-Lycian Block at ~125–85 Mya, there was a distinct time gap of at least 20 Ma in arc-related magmatism and high-P metamorphism before the subduction of the Pindos Oceanic Unit began at ~60 Mya. The latter age is also broadly constrained by flysch deposition in the Cycladic Blueschist Unit and the development of the Meso-Hellenic and Thrace forearc basins.

We argue that the time gap shows a marked slow-down or even a halt of subduction between ~85 and 60 Mya, followed by a renewed phase of subduction when the Pindos Oceanic Unit entered the subduction zone. Whether or not a new subduction zone formed near the Mesozoic subduction zone (Ricou et al. 1998) is possibly beyond the resolution of the existing tomographic images. Nevertheless, the subduction and accretion of the Pindos Oceanic Unit caused a distinct change in the dynamics of the subduction zone, and the system changed from advancing/stationary to retreating at some time near 55–50 Mya.

Ring & Layer (2003) and Brun & Faccenna (2008) showed that the arrival of continental fragments in the Cenozoic subduction zone caused punctuated high-P accretion events that were superimposed on southward rollback of the subduction zone. Several high-P metamorphic events can be distinguished in space and time. Evidence for the earliest high-P metamorphism of ~53 Mya is recorded in the ophiolitic Selçuk Mélange and basement-cover succession in the northern Cycladic Blueschist Unit (e.g., Syros, Samos). The structurally deeper levels became accreted later, and as a consequence, the high-P metamorphism occurred at a later time. Although there are gaps in the spatial coverage of the age of high-P metamorphism, the data show that high-P subduction-zone-related metamorphism becomes progressively younger to the south of the Aegean, reflecting the southward retreat of the Hellenic slab. The similarity in the shape and direction of the P-T paths inferred for various units on several Aegean islands is considered strong evidence for a remarkably steady-state thermal profile of the southward-retreating subduction zone from ~55–50 to ~25–20 Mya.

Possible Role of the 660-km Discontinuity for Slab Rollback

As discussed above, the 660-km discontinuity is important for the fate of the subducting slab (Ringwood 1991). Owing to their density, viscosity, and rate of subduction, some slabs do not

immediately penetrate the 660-km discontinuity but are instead deflected horizontally along the upper/lower mantle boundary (Ringwood 1991, Schellart 2005).

Faccenna et al. (2003) and van Hinsbergen et al. (2005) showed that the Jurassic/Cretaceous slab penetrated through the 660-km discontinuity. There is agreement that tomography shows a ~ 300 -km horizontal portion of the slab just above the 660-km discontinuity (van Hinsbergen et al. 2005). The value of ~ 300 km is identical to the estimate for Cenozoic extension of ~ 320 km (Faccenna et al. 2003).

As summarized above, Faccenna et al. (2003) showed that the upper-mantle high-velocity anomaly reflects Cenozoic subduction of the Hellenic slab. In other words, the Cenozoic portion of the slab has not penetrated through the 660-km discontinuity and is draped over it for ~ 300 km (van Hinsbergen et al. 2005). One can only speculate about when the Cenozoic slab reached the 660-km discontinuity. For a subduction angle of 30 – 40° and an average subduction rate of 30 km Ma^{-1} , it would take the slab ~ 35 – 40 Ma to reach the 660-km boundary. Given that subduction of the Pindos Oceanic Unit commenced at ~ 60 Mya, the slab may have reached the upper/lower mantle transition at some time between 25 and 20 Mya. As the petrologic and geochronologic data imply a fairly steady-state process until ~ 25 – 20 Mya, these data support the proposition that the slab reached the 660-km discontinuity at ~ 25 – 20 Mya. Although this age estimate is anything but precise, it is interesting that it coincides with the initiation of Aegean-wide large-scale extension at 23–19 Mya, the ensuing opening of the Aegean Sea basin, and the distinct thermal anomaly in the Naxos/Paros-Ios region. At approximately this time (i.e., 25–20 Mya), the rate of convergence between Africa and Eurasia slowed down again (Dewey et al. 1989, Rosenbaum et al. 2002). We propose that these coincidences are not fortuitous. As the portion of the Hellenic slab composed of the Pindos Oceanic Unit and the units to the south of it reached the 660-km discontinuity and was draped over it, possibly aided by a decrease in the rate of plate convergence (Faccenna et al. 2003), the resulting increase in slab retreat appears to have taken away the abutment that kept the Aegean lithosphere together. This event triggered a major phase of Aegean-wide extension (as schematically sketched in **Figure 3**). The resulting lithospheric thinning and increased flow in the asthenosphere were greatest in the center of the extending domain and may have caused the thermal anomaly in the Naxos/Paros-Ios region a few Ma later.

As shown above, Aegean-wide extension starting at 23–19 Mya does not show a distinct spatial age distribution. We suggest that this extension phase therefore differed from the rather continuous southward retreat of the Hellenic slab that caused the age pattern of the high-P rocks. Instead, we envision that the draping of the Hellenic slab over the 660-km discontinuity correlated with a period of enhanced rollback and triggered ~ 300 km of rapid and pervasive extension across the entire Aegean. The tear in the slab beneath western Turkey as suggested by de Boorder et al. (1998) probably partly accommodated the fast rollback of the slab in the Aegean Sea region (**Figure 6**). If so, the tear would have started to form at 23–19 Mya.

Low-Angle Normal Faulting and Reactivation of the Former Subduction Thrust

The basal thrusts of extrusion wedges commonly are relatively shallow-level segments of the subduction thrust. The thrusts typically have dip angles of $\leq 30^\circ$. The geometry of an extrusion wedge requires that the normal faults at the top of the wedge dip at similar shallow angles and hence are low-angle normal faults. Ring et al. (2007b) argued that segments of earlier subduction thrusts were reactivated as normal-sense shear zones as subduction retreated outboard. Outboard

retreat of the subduction thrust was in most cases probably forced by an incoming fragment of continental crust. The extrusion wedges on Evia and Samos/western Turkey provide examples for that. In both cases the extrusion wedge is composed of rocks of the continental basement-cover sequence of the Cycladic Blueschist Unit, and the entire ophiolitic Selçuk Mélange acted as a rheologically heterogeneous normal shear zone that constitutes the top of the extrusion wedges. The reactivation of the former subduction thrust as a normal fault also highlights the importance of reactivation of preexisting structures in the development of low-angle normal faults (cf. Axen 2004).

SUMMARY POINTS

1. High-P metamorphism related to subduction of the Cenozoic Hellenic slab started at ~53 Mya in the northern Cyclades and shifted progressively southward to where high-P rocks are forming underneath Crete today. The underthrusting of fragments of (thinned) continental crust might have resulted in episodes of punctuated exhumation of high-P rocks during continued retreat/rollback of the subducting slab.
2. Available petrologic data and the inferred P-T paths strongly suggest that the retreating Cenozoic Hellenic subduction zone reached steady-state thermal conditions, with low average geothermal gradients in the suprasubduction zone crust, soon after inception of subduction of the Pindos Oceanic Unit at ~60 Mya. There is no indication that these conditions changed in any significant way until ~25–20 Mya. The latter is approximately the time when we estimate that the Cenozoic portion of the slab was draped over the 660-km discontinuity, and the time of onset of large-scale extension across the entire Aegean region. We propose that the draping of the slab over the 660-km discontinuity resulted in accelerated slab retreat and that it provides a cause for ~300 km of extension and the ensuing opening of the Aegean Sea basin. Possible tearing of the slab would be a result of fast, spatially restricted rollback in the Aegean Sea region.
3. Despite the fact that the tomographic data are commonly interpreted to reflect continuous subduction since ~200 Mya, we suggest a couple of major temporal discontinuities: (a) a time gap before subduction of the Pindos Oceanic Unit and (b) different styles of slab subduction after the inception of Cenozoic subduction of the Pindos Oceanic Unit with rollback-related extension of the overriding plate.
4. The bulk exhumation of the Cycladic Blueschist Unit and the high-P belt on Crete occurred primarily in a forearc position. Most of the exhumation of the high-P rocks in the Cyclades and Crete occurred relatively soon after the rocks experienced high-P conditions. The syn-subduction exhumation took place in extrusion wedges. Early exhumation in extrusion wedges does not appear to have been important for the high-P rocks within the thermal anomaly in the Naxos/Paros-Ios region.
5. On Naxos (and Ios), large-scale (bivergent) extension from >21 to 8 Mya accomplished 30–35 km of exhumation of amphibolite- to granulite-facies high-T rocks and caused a distinct thermal anomaly in the central Aegean.
6. The distinction between shortening- and extension-related normal faults is important, especially when it comes to constraining the timing of inception of large-scale extension in the Aegean. The latter cannot necessarily be constrained by dating normal faults alone.

FUTURE ISSUES

1. How widespread are extrusion wedges in the Aegean and other subduction complexes? Critical for proving the existence of an extrusion wedge is the contemporaneity of slip on the basal thrust faults and the upper normal fault. A related question is, At what time in the orogenic history does thickened crust start to become significantly attenuated? Attenuation may not develop when thrust and shortening-related normal faults are active in concert. In other words, the crust will not necessarily be extended and attenuated during exhumation of high-P rocks in extrusion wedges.
2. A major problem in the Aegean is the heat source driving the Naxos/Paros-Ios thermal anomaly. One possible solution entails large-scale lower crustal flow drawing hot material into the most highly extended region from the base of the surrounding crust. Such a scenario would demand high-strain flow zones in the high-temperature metamorphic rocks and could be tested by strain analysis in the high-temperature rocks. Another possible solution involves magmatic underplating to the base of thinned continental crust, causing elevated heat and fluid flow. This scenario would be testable through the discovery of early Miocene mafic melts on Naxos or through a deep geophysical survey aimed at finding a mafic underplate. Note that both scenarios are not mutually exclusive.
3. Constraining the nature and especially the timing of greenschist-facies metamorphic processes is critical to understanding exhumation dynamics.
4. Exact rates and displacements for the extensional detachments are important for deciphering whether large-scale extension in the Aegean is indeed resolved along a few major extensional structures as schematically depicted in **Figure 7**.
5. The Cretan detachment is an important structure and the east-to-west younging of ZFT ages needs to be understood. The critical question is whether there is more than one single detachment fault or whether a single Cretan detachment has an unusual geometry.
6. The regional pattern of fission-track ages needs to be refined. In addition, similar cooling-age maps based on zircon and apatite (U-Th)/He ages should be constructed. Well-defined regional cooling maps will aid tectonic interpretations of the spatial and temporal pattern of extension in the Aegean. A deeper understanding of processes will be gained only if the geometry and the timing of large-scale extension are well known.
7. We have shown that there is a temporal relationship between draping of the Cenozoic slab over the 660-km discontinuity and large-scale Aegean extension. It would be worthwhile to compare the Hellenic subduction zone with other retreating subduction zones worldwide to detect similar relationships, which would corroborate our hypothesis.

DISCLOSURE STATEMENT

The authors are not aware of any affiliations, memberships, funding, or financial holdings that might be perceived as affecting the objectivity of this review.

ACKNOWLEDGMENTS

This work was supported in part by grants from the Deutsche Forschungsgemeinschaft (Ri 538/16, /18, and /23), by the New Zealand Brian Mason trust (grant E5345), and by the College of Science

of Canterbury University. We thank Othmar Müntener, Gianreto Manatschal, Djordje Grujic, Rick Law, Oliver Jagoutz, and Virginia Toy for various helpful comments. Kevin Burke provided thorough and critical reviews, which helped considerably to improve the paper. Editorial handling by Nina Perry, Sayzie Koldys, and Jennifer Jongsma is greatly appreciated.

LITERATURE CITED

- Altherr R, Schliestedt M, Okrusch M, Seidel E, Kreuzer H, et al. 1979. Geochronology of high-pressure rocks on Sifnos (Cyclades, Greece). *Contrib. Mineral. Petrol.* 70:245–55
- Avigad D. 1998. High-pressure metamorphism and cooling on SE Naxos (Cyclades, Greece). *Eur. J. Mineral.* 10:1309–19
- Avigad D, Garfunkel Z. 1991. Uplift and exhumation of high-pressure metamorphic terrains: the example of the Cycladic blueschist belt (Aegean Sea). *Tectonophysics* 188:357–72
- Avigad D, Garfunkel Z, Jolivet L, Azañon JM. 1997. Back arc extension and denudation of Mediterranean eclogites. *Tectonics* 16:924–41
- Axen GJ. 2004. Mechanics of low-angle normal faults. In *Rheology and Deformation in the Lithosphere at Continental Margins*, ed. G Karner, B Taylor, N Driscoll, DL Kohlstedt, pp. 46–91. New York: Columbia Univ. Press
- Barr SR, Temperley S, Tarney J. 1999. Lateral growth of the continental crust through deep level subduction-accretion: a re-evaluation of central Greek Rhodope. *Lithos* 46:69–94
- Bijwaard H, Spakman W, Engdahl ER. 1998. Closing the gap between regional and global travel time tomography. *J. Geophys. Res.* 103:30055–78
- Böger H. 1983. Stratigraphische und tektonische Verknüpfungen kontinentaler Sedimente des Neogens im Ägäis-Raum. *Geol. Rundsch.* 72:771–814
- Bolhar R, Ring U, Allen CM. 2010. An integrated zircon geochronological and geochemical investigation into the Miocene plutonic evolution of the Cyclades, Aegean Sea, Greece: Part 1—Geochronology. *Contrib. Mineral. Petrol.* In press, doi:10.1007/s00410-010-0504-4
- Bonev N, Beccaleto L. 2007. From syn- to post-orogenic Tertiary extension in the north Aegean region: constraints on the kinematics in the eastern Rhodope–Thrace, Bulgaria–Greece and the Biga Peninsula, NW Turkey. *Geol. Soc. London Spec. Publ.* 291:113–42
- Bonev N, Marchev P, Singer B. 2006. $^{40}\text{Ar}/^{39}\text{Ar}$ geochronology constraints on the Middle Tertiary basement extensional exhumation and its relation to ore-forming and magmatic processes in the eastern Rhodope (Bulgaria). *Geodin. Acta* 19:267–82
- Bonneau M. 1984. Correlation of the Hellenide nappes in the southeast Aegean and their tectonic reconstruction. *Geol. Soc. London Spec. Publ.* 17:517–27
- Brichau S, Ring U, Carter A, Bolhar R, Monié P, et al. 2008. Timing, slip rate, displacement and cooling history of the Mykonos detachment footwall, Cyclades, Greece, and implications for the opening of the Aegean Sea basin. *J. Geol. Soc. London* 165:263–77
- Brichau S, Ring U, Carter A, Monié P, Bolhar R, et al. 2007. Extensional faulting on Tinos Island, Aegean Sea, Greece: How many detachments? *Tectonics* 26:TC4009
- Brichau S, Ring U, Ketcham R, Carter A, Stockli D, Brunel M. 2006. Constraining the long-term evolution of the slip rate for a major extensional fault system in the central Aegean, Greece, using thermochronology. *Earth Planet. Sci. Lett.* 241:293–306
- Brichau S, Thomson S, Ring U. 2010. Thermochronometric constraints on the tectonic evolution of the Serifos detachment, Aegean Sea, Greece. *Int. J. Earth Sci.* 99:379–93
- Brix MR, Stöckhert B, Seidel E, Theye T, Thomson SN, Küster M. 2002. Thermobarometric data from a fossil zircon partial annealing zone in high pressure–low temperature rocks of eastern and central Crete, Greece. *Tectonophysics* 349:309–26
- Bröcker M, Kreuzer H, Matthews A, Okrusch M. 1993. $^{40}\text{Ar}/^{39}\text{Ar}$ and oxygen isotope studies of polymetamorphism from Tinos Island, Cycladic blueschist belt, Greece. *J. Metamorph. Geol.* 11:223–40
- Brun J-P, Faccenna C. 2008. Exhumation of high-pressure rocks driven by slab rollback. *Earth Planet. Sci. Lett.* 272:1–7

- Büttner D, Kowalczyk G. 1978. Late Cenozoic stratigraphy and paleogeography of Greece—a review. In *Alps, Apennines, Hellenides: Geodynamic Investigation along Geotraverses by an International Group of Geoscientists*, ed. H Closs, D Roeder, K Schmidt, pp. 494–501. IUCG. Sci. Rep. 38. Stuttgart: Schweizerbart
- Buick IS. 1991. The late Alpine evolution of an extensional shear zone, Naxos, Greece. *J. Geol. Soc. London* 148:93–103
- Buick IS, Holland TJB. 1989. The P - T - t path associated with crustal extension, Naxos, Cyclades, Greece. *Geol. Soc. London Spec. Publ.* 43:365–69
- Chase CG. 1979. Subduction, the geoid, and lower mantle convection. *Nature* 282:464–68
- Chase CG. 1980. Extension behind island arcs and motions relative to hot spots. *J. Geophys. Res.* 83:5385–87
- de Boorder H, Spakman W, White SH, Wortel MJR. 1998. Late Cenozoic mineralization, orogenic collapse and slab detachment in the European Alpine Belt. *Earth Planet Sci. Lett.* 164:569–75
- de Sigoyer J, Guillot S, Dick P. 2004. Exhumation of the ultrahigh-pressure Tso Moriri unit in eastern Ladakh (NW Himalaya): a case study. *Tectonics* 23:TC3003
- Dewey JF, Bird JM. 1970. Mountain belts and new global tectonics. *J. Geophys. Res.* 75:2625–47
- Dewey JF, Helman ML, Torco E, Hutton DHW, Knott SD. 1989. Kinematics of the western Mediterranean. *Geol. Soc. London Spec. Publ.* 45:265–83
- Dinter DA. 1998. Late Cenozoic extension of the Alpine collisional orogen, northeastern Greece: origin of the north Aegean basin. *Geol. Soc. Am. Bull.* 110:1208–30
- Doutsos T, Koukouvelas I, Poulimenos G, Kokkolas S, Xypolias P, Skourlis K. 2000. An exhumation model of the south Peloponnesus, Greece. *Int. J. Earth Sci.* 89:350–65
- Duchêne S, Aissa R, Vanderhaeghe O. 2006. Pressure-temperature-time evolution of metamorphic rocks from Naxos (Cyclades, Greece): constraints from thermobarometry and Rb/Sr dating. *Geodin. Acta* 19:301–21
- Duermeijer CE, Nyst M, Meijer PT, Langereis CG, Spakman W. 2000. Neogene evolution of the Aegean arc: paleomagnetic and geodetic evidence for a rapid and young rotation phase. *Earth Planet. Sci. Lett.* 176:509–25
- Dürr S, Altherr R, Keller J, Okrusch M, Seidel E. 1978. The median Aegean crystalline belt: stratigraphy, structure, metamorphism, magmatism. In *Alps, Apennines, Hellenides: Geodynamic Investigation along Geotraverses by an International Group of Geoscientists*, ed. H Closs, D Roeder, K Schmidt, pp. 537–64. IUCG. Sci. Rep. 38. Stuttgart: Schweizerbart
- Elsasser WM. 1971. Sea-floor spreading as thermal convection. *J. Geophys. Res.* 76:1101–12
- Faccenna C, Jolivet L, Piromallo C, Morelli A. 2003. Subduction and the depth of convection in the Mediterranean mantle. *J. Geophys. Res.* 108(B2):2099
- Fassoulas C, Kiliass A, Mountrakis D. 1994. Postnappe stacking extension and exhumation of high-pressure/low-temperature rocks in the island of Crete, Greece. *Tectonics* 13:127–38
- Forster MA, Lister GS. 2005. Several distinct tectono-metamorphic slices in the Cycladic eclogite-blueschist belt, Greece. *Contrib. Mineral. Petrol.* 150:523–45
- Funicello F, Faccenna C, Giardini D, Regenauer-Lieb K. 2003. Dynamics of retreating slabs: 2. Insights from three-dimensional laboratory experiments. *J. Geophys. Res.* 108(B4):2207
- Fytikas M, Innocenti F, Manetti P, Mazuoli R, Peccerillo A, Villari L. 1984. Tertiary to Quaternary evolution of volcanism in the Aegean region. *Geol. Soc. London Spec. Publ.* 17:687–700
- Garfunkel Z, Anderson CA, Schubert G. 1986. Mantle circulation and the lateral migration of subducted slabs. *J. Geophys. Res.* 91:7205–23
- Gautier P, Ballèvre M, Brun J-P, Jolivet L. 1990. Extension ductile et bassins sédimentaires mio-pliocènes dans les Cyclades (îles de Naxos et Paros). *C. R. Acad. Sci.* 310:147–53
- Glodny J, Ring U, Kühn A, Gleissner P, Franz G. 2005. Crystallization and very rapid exhumation of the youngest Alpine eclogites (Tauern Window, Eastern Alps) from Rb/Sr mineral assemblage analysis. *Contrib. Mineral. Petrol.* 149:699–712
- Godfriaux I. 1968. Etude géologique de la région de l'Olympe (Grèce). *Ann. Geol. Pays Hell.* 19:1–271
- Grasemann B, Petrakakis K. 2007. Evolution of the Serifos metamorphic core complex. *J. Virtual Explor.* 27:2, doi:10.3809/jvirtex.2007.00170
- Grütter HS. 1993. *Structural and metamorphic studies on Ios, Cyclades, Greece*. PhD thesis. Univ. Cambridge. 227 pp.

- Hatzfeld D. 1994. On the shape of the subducting slab beneath the Peloponnese, Greece. *Geophys. Res. Lett.* 21:173–76
- Hejl E, Riedl H, Weingartner H. 2002. Post-plutonic unroofing and morphogenesis of the Attic-Cycladic complex (Aegea, Greece). *Tectonophysics* 349:37–56
- Henjes-Kunst F, Altherr R, Kreuzer H, Hansen BT. 1988. Disturbed U-Th-Pb systematics of young zircons and uranotorites: the case of the Miocene Aegean granitoids (Greece). *Chem. Geol.* 73:125–45
- Huvaz O, Karahanoglu N, Ediger V. 2007. The thermal gradient history of the Thrace Basin, NW Turkey: correlation with basin evolution processes. *J. Petrol. Geol.* 30:3–24
- Isacks B, Molnar P. 1969. Mantle earthquake mechanisms and sinking of lithosphere. *Nature* 223:1121–24
- Jacobshagen V. 1986. *Geologie von Griechenland*. Berlin: Gebrüder Borntraeger. 636 pp.
- Jansen JBH. 1973. 1: 50 000 Geological map of Naxos. Institute of Geological and Mineral Exploration, Athens.
- Jansen JBH, Schuiling RD. 1976. Metamorphism on Naxos: petrology and geothermal gradients. *Am. J. Sci.* 276:1225–53
- John BE, Howard KA. 1995. Rapid extension recorded by cooling-age patterns and brittle deformation, Naxos, Greece. *J. Geophys. Res.* 100:9969–79
- Jolivet L, Brun J-P. 2010. Cenozoic geodynamic evolution of the Aegean. *Int. J. Earth Sci.* 99:109–38
- Jolivet L, Goffé B, Monié P, Truffert-Luxey C, Patriat M, Bonneau M. 1996. Miocene detachment in Crete and exhumation P-T-t paths of high-pressure metamorphic rocks. *Tectonics* 15:1129–53
- Katzir Y, Avigad D, Matthews A, Garfunkel Z, Evans BW. 2000. Origin, PP/LT metamorphism and cooling of ophiolitic mélanges in southern Evia (NW Cyclades), Greece. *J. Metamorph. Geol.* 18:699–718
- Keay S. 1998. *The geological evolution of the Cyclades, Greece: constraints from SHRIMP U-Pb geochronology*. PhD thesis. Aust. Natl. Univ., Canberra. 335 pp.
- Keay S, Lister G, Buick I. 2001. The timing of partial melting, Barrovian metamorphism and granite intrusion in the Naxos metamorphic core complex, Cyclades, Aegean Sea, Greece. *Tectonophysics* 342:275–312
- Kincaid C, Griffiths RW. 2003. Thermal evolution of the mantle during rollback subduction. *Nature* 425:58–62
- Knapmeyer M, Harjes H-P. 2000. Imaging crustal discontinuities and the downgoing slab beneath western Crete. *Geophys. J. Int.* 143:1–21
- Kopf A, Mascle J, Klaeschen D. 2003. The Mediterranean Ridge: a mass balance across the fastest growing accretionary complex on Earth. *J. Geophys. Res.* 108(B8):2372
- Kounov A, Seward D, Bernoulli D, Burg JP, Ivanov Z. 2004. Thermotectonic evolution of an extensional dome: the Cenozoic Osogovo-Lisets core complex (Kraishte zone, western Bulgaria). *Int. J. Earth Sci.* 93:1008–24
- Krohe A, Mposkos E. 2002. Multiple generations of extensional detachments in the Rhodope Mountains (northern Greece): evidence of episodic exhumation of high-pressure rocks. *Geol. Soc. London Spec. Publ.* 204:151–78
- Kuhlemann J, Frisch W, Dunkl I, Kazmer M, Schmiedl G. 2004. Miocene siliciclastic deposits of Naxos Island: geodynamic and environmental implications for the evolution of the southern Aegean Sea (Greece). *Geol. Soc. Am. Spec. Pap.* 378:51–65
- Kumerics C, Ring U, Brichau S, Glodny J, Monié P. 2005. The extensional Messaria shear zone and associated brittle detachment faults, Aegean Sea, Greece. *J. Geol. Soc. London* 162:701–21
- Lee J, Lister GS. 1992. Late Miocene ductile extension and detachment faulting, Mykonos, Greece. *Geology* 20:121–24
- Lips ALW, Wijbrans JR, White SH. 1999. New insights from $^{40}\text{Ar}/^{39}\text{Ar}$ laserprobe dating of white mica fabrics from the Pelion Massif, Pelagonian Zone, Internal Hellenides, Greece: implications for the timing of metamorphic episodes and tectonic events in the Aegean region. *Geol. Soc. London Spec. Publ.* 156:457–74
- Lister GS, Banga G, Feenstra A. 1984. Metamorphic core complexes of Cordilleran type in the Cyclades, Aegean Sea, Greece. *Geology* 12:21–25
- Lister GS, Raouzaïos A. 1996. The tectonic significance of a porphyroblastic blueschist facies overprint during Alpine orogenesis: Sifnos, Aegean Sea, Greece. *J. Struct. Geol.* 18:1417–35
- Loneragan L, White N. 1997. Origin of the Betic-Rif mountain belt. *Tectonics* 16:504–22
- Long MD, Silver PG. 2008. The subduction zone flow field from seismic anisotropy: a global view. *Science* 319:315–18

- Makris J, Stobbe C. 1984. Physical properties and state of the crust and upper mantle of the Eastern Mediterranean Sea deduced from geophysical data. *Marine Geol.* 55:347–63
- Maluski H, Vergely P, Bavay D, Bavay P, Katsikatos G. 1981. $^{39}\text{Ar}/^{40}\text{Ar}$ dating of glaucophanes and phengites in southern Euboa (Greece) geodynamic implications. *Bull. Soc. Geol. Fr.* 23:469–76
- Marchev P, Raicheva R, Downes H, Vaselli O, Chiaradia M, Moritz R. 2004. Compositional diversity of Eocene–Oligocene basaltic magmatism in the Eastern Rhodopes, SE Bulgaria: implications for genesis and tectonic setting. *Tectonophysics* 393:301–28
- Meier T, Becker D, Endrun B, Rische M, Bohnhoff M, et al. 2007. A model for the Hellenic subduction zone in the area of Crete based on seismological investigations. *Geol. Soc. London Spec. Publ.* 291:183–99
- Meulenkamp JE, Wortel MJR, van Wamel WA, Spakman W, Hoogerduyn-Strating E. 1988. On the Hellenic subduction zone and the geodynamic evolution of Crete since the late middle Miocene. *Tectonophysics* 146:203–15
- Mposkos E, Kostopoulos DK. 2001. Diamond, former coesite and supersilicic garnet in metasedimentary rocks from the Greek Rhodope: a new ultrahigh-pressure metamorphic province established. *Earth Planet. Sci. Lett.* 192:497–506
- Okrusch M, Bröcker M. 1990. Eclogites associated with high-grade blueschists in the Cyclades archipelago, Greece: a review. *Eur. J. Mineral.* 2:451–78
- Ovtcharova M, von Quadt A, Cherneva Z, Peytcheva I, Heinrich CA, et al. 2003. Isotope and geochronological study on magmatism and migmatization in the central Rhodopian core complex, Bulgaria. In *Geodynamics and Ore Deposit Evolution of the Alpine–Balkan–Carpathian–Dinaride Province, ABCD–GEODE Workshop Proc., Seggau, Austria*, ed. F Neubauer, R Handler, p. 42
- Özer S, Sözbilir H, Özkar I, Toker V, Sari B. 2001. Stratigraphy of Upper Cretaceous–Palaeogene sequences in the southern and eastern Menderes Massif (Western Turkey). *Int. J. Earth Sci.* 89:852–66
- Papazachos C, Nolet G. 1997. Deep velocity structure of the Hellenic area obtained by robust nonlinear inversion of travel times. *J. Geophys. Res.* 102:8349–67
- Pe-Piper G, Piper DJW. 2002. *The Igneous Rocks of Greece: The Anatomy of an Orogen*. Berlin: Gebrüder Borntraeger. 573 pp.
- Putlitz B, Cosca MA, Schumacher JC. 2005. Prograde mica $^{40}\text{Ar}/^{39}\text{Ar}$ growth ages recorded in high pressure rocks (Syros, Cyclades, Greece). *Chem. Geol.* 214:79–98
- Reddy SM, Wheeler J, Cliff RA. 1999. The geometry and timing of orogenic extension: an example from the western Italian Alps. *J. Metamorph. Geol.* 17:573–89
- Reiners PW, Brandon MT. 2006. Using thermochronology to understand orogenic erosion. *Annu. Rev. Earth Planet. Sci.* 34:419–66
- Ricou LE, Burg JP, Godfriaux I, Ivanov Z. 1998. Rhodope and Vardar: the metamorphic and the olistostromic paired belts related to the Cretaceous subduction under Europe. *Geodin. Acta* 11:285–309
- Ring U, Glodny J. 2010. No need for lithospheric extension for exhuming (U)HP rocks by normal faulting. *J. Geol. Soc. London* 167:225–28, doi:10.1144/0016-76492009-134
- Ring U, Glodny J, Will T, Thomson S. 2007a. An Oligocene extrusion wedge of blueschist-facies nappes on Evia, Aegean Sea, Greece: implications for the early exhumation of high-pressure rocks. *J. Geol. Soc. London* 164:637–52
- Ring U, Layer PW. 2003. High-pressure metamorphism in the Aegean, eastern Mediterranean: underplating and exhumation from the Late Cretaceous until the Miocene to recent above the retreating Hellenic subduction zone. *Tectonics* 22(3):1022
- Ring U, Layer PW, Reischmann T. 2001. Miocene high-pressure metamorphism in the Cyclades and Crete, Aegean Sea, Greece: evidence for large-magnitude displacement on the Cretan detachment. *Geology* 29:395–98
- Ring U, Reischmann T. 2002. The weak and superfast Cretan detachment, Greece: exhumation at subduction rates in extrusion wedges. *J. Geol. Soc. London* 159:225–28
- Ring U, Thomson SN, Bröcker M. 2003. Fast extension but little exhumation: the Vari detachment in the Cyclades, Greece. *Geol. Mag.* 140:245–52
- Ring U, Thomson SN, Rosenbaum G. 2009. Timing of the Amorgos detachment system and implications for detachment faulting in the southern Aegean Sea, Greece. *Geol. Soc. London Spec. Publ.* 321:169–77

- Ring U, Will T, Glodny J, Kumerics C, Gessner K, et al. 2007b. Early exhumation of high-pressure rocks in ex-trusion wedges: Cycladic blueschist unit in the eastern Aegean, Greece, and Turkey. *Tectonics* 26:TC2001
- Ringwood AE. 1991. Phase transformations and their bearing on the constitution and dynamics of the mantle. *Geochim. Cosmochim. Acta* 55:2083–110
- Robertson AHF, Clift PD, Degnan PJ, Jones G. 1991. Paleogeographic and paleotectonic evolution of the eastern Mediterranean Neotethys. *Palaeogeogr. Palaeoclimatol. Palaeoecol.* 87:289–343
- Robertson AHF, Dixon JE, Brown S, Collins A, Morris A, Pickett E. 1996. Alternative tectonic models for the Late Palaeozoic–Early Tertiary development of Tethys in the eastern Mediterranean region. *Geol. Soc. London Spec. Publ.* 105:239–63
- Rosenbaum G, Lister GS, Duboz C. 2002. Relative motion of Africa, Iberia and Europe during Alpine orogeny. *Tectonophysics* 359:117–29
- Rosenbaum G, Ring U, Kühn A. 2007. Tectonometamorphic evolution of high-pressure rocks from the island of Amorgos (Central Aegean, Greece). *J. Geol. Soc. London* 164:425–38
- Royden LH. 1993. Evolution of retreating subduction boundaries formed during continental collision. *Tectonics* 12:629–38
- Royden LH, Husson L. 2006. Trench motion, slab geometry and viscous stresses in subduction systems. *Geophys. J. Int.* 167:881–905
- Sánchez-Gómez M, Avigad D, Heimann A. 2002. Geochronology of clasts in allochthonous Miocene sedimentary sequences on Mykonos and Paros Islands: implications for back-arc extension in the Aegean Sea. *J. Geol. Soc. London* 159:45–60
- Schellart WP. 2005. Influence of the subducting plate velocity on the geometry of the slab and migration of the subduction hinge. *Earth Planet. Sci. Lett.* 231:197–219
- Schermer ER, Lux DR, Burchfiel BC. 1990. Temperature-time history of subducted continental crust, Mount Olympus region, Greece. *Tectonics* 9:1165–95
- Schmädicke E, Will TM. 2003. Pressure-temperature evolution of blueschist facies rocks from Sifnos, Greece, and implications for the exhumation of high-pressure rocks in the central Aegean. *J. Metamorph. Geol.* 21:799–811
- Seidel E, Kreuzer H, Harre W. 1982. A late Oligocene/early Miocene high pressure belt in the External Hellenides. *Geol. Jahrb.* E23:165–206
- Şengör AMC, Tüysüz O, İmren C, Sakiç M, Eyidoğan H, et al. 2005. The North Anatolian Fault: a new look. *Annu. Rev. Earth Planet. Sci.* 33:37–112
- Seward D, Vanderhaeghe O, Siebenaller L, Thomson SN, Hibsich C, et al. 2009. Cenozoic tectonic evolution of Naxos Island through a multi-faceted approach of fission-track analysis. *Geol. Soc. London Spec. Publ.* 321:179–96
- Shaked Y, Avigad D, Garfunkel Z. 2000. Alpine high-pressure metamorphism at the Almyropotamos window (southern Evia, Greece). *Geol. Mag.* 137:367–80
- Sherlock S, Kelley SP, Inger S, Harris N, Okay AI. 1999. ⁴⁰Ar-³⁹Ar and Rb-Sr geochronology of high-pressure metamorphism and exhumation history of the Tavsanli Zone, NW Turkey. *Contrib. Mineral. Petrol.* 137:46–58
- Sotiropoulos S, Kamberis E, Triantaphyllou M, Doutsos T. 2003. Thrust sequences in the central part of the External Hellenides. *Geol. Mag.* 140:661–68
- Spakman W, Van Der Lee S, Van Der Hilst R. 1993. Travel-time tomography of the European–Mediterranean mantle down to 1400 km. *Phys. Earth Planet. Interiors* 79:3–74
- Thomson SN, Ring U, Brichau S, Glodny J, Will TM. 2009. Timing and nature of formation of the Ios metamorphic core complex, southern Cyclades, Greece. *Geol. Soc. London Spec. Publ.* 321:139–67
- Thomson SN, Stöckhert B, Brix MR. 1998a. Thermochronology of the high-pressure metamorphic rocks of Crete, Greece: implications for the speed of tectonic processes. *Geology* 26:259–62
- Thomson SN, Stöckhert B, Brix MR. 1999. Miocene high-pressure metamorphic rocks of Crete, Greece: rapid exhumation by buoyant escape. *Geol. Soc. London Spec. Publ.* 154:87–108
- Thomson SN, Stöckhert B, Rauche H, Brix MR. 1998b. Apatite fission-track thermochronology of the uppermost tectonic unit of Crete, Greece: implications for the post-Eocene tectonic evolution of the Hellenic Subduction System. In *Advances in Fission-Track Geochronology*, ed. P Van den Haute, F De Corte, pp. 187–205. Dordrecht, The Netherlands: Kluwer Acad.

- Tomaschek F, Kennedy A, Villa IM, Lagos M, Ballhaus C. 2003. Zircons from Syros, Cyclades, Greece—recrystallization and mobilisation during high-pressure metamorphism. *J. Petrol.* 44:1977–2002
- Trotet F, Jolivet L, Vidal O. 2001. Tectono-metamorphic evolution of Syros and Sifnos islands (Cyclades, Greece). *Tectonophysics* 338:179–206
- Uyeda S. 1982. Subduction zones: an introduction to comparative subductology. *Tectonophysics* 81:133–59
- Vamvaka A, Kiliadis AD, Mountrakis D, Papoikononou J. 2006. Geometry and structural evolution of the Mesohellenic Trough (Greece): a new approach. *Geol. Soc. London Spec. Publ.* 260:521–38
- Vanderhaeghe O, Hibsich C, Siebenaller L, Duchêne S, de St Blanquat M, et al. 2007. Penrose conference—extending a continent—Naxos field guide. *J. Virtual Explor.* 27:4, doi:10.3809/jvirtex.2007.00175
- van Hinsbergen DJJ, Hafkenscheid E, Spakman W, Meulenkamp JE, Wortel R. 2005. Nappe stacking resulting from subduction of oceanic and continental lithosphere below Greece. *Geology* 33:325–28
- van Hinsbergen DJJ, Van Der Meer DG, Zachariasse WJ, Meulenkamp JE. 2006. Deformation of western Greece during Neogene clockwise rotation and collision with Apulia. *Int. J. Earth Sci.* 95:463–90
- von Quadt A, Moritz R, Peytcheva I, Heinrich CA. 2005. Geochronology and geodynamics of Late Cretaceous magmatism and Cu-Au mineralization in the Panagyurishte region of the Apuseni-Banat-Timok-Srednogie belt, Bulgaria. *Ore Geol. Rev.* 27:95–126
- Wawrzenitz N, Krohe A. 1998. Exhumation and doming of the Thasos metamorphic core complex (S Rhodope, Greece): structural and geochronological constraints. *Tectonophysics* 285:301–32
- Wijbrans JR, McDougall I. 1988. Metamorphic evolution of the Attic Cycladic metamorphic belt on Naxos (Cyclades, Greece) utilizing $^{40}\text{Ar}/^{39}\text{Ar}$ age spectrum measurements. *J. Metamorph. Geol.* 6:571–94
- Wijbrans JR, Schliestedt N, York D. 1990. Single grain argon laser probe dating of phengites from the blueschist to greenschist transition on Sifnos (Cyclades, Greece). *Contrib. Mineral. Petrol.* 104:582–93
- Will T, Okrusch M, Schmädicke E, Chen G. 1998. Phase relations in the greenschist-blueschist-amphibolite-eclogite facies in the system $\text{Na}_2\text{O}-\text{CaO}-\text{FeO}-\text{MgO}-\text{Al}_2\text{O}_3-\text{SiO}_2-\text{H}_2\text{O}$ (NCFMASH), with application to metamorphic rocks from Samos, Greece. *Contrib. Mineral. Petrol.* 132:85–102



Annual Review
of Earth and
Planetary Sciences

Volume 38, 2010

Contents

| | |
|---|-----|
| Frontispiece | |
| <i>Ikuo Kushiro</i> | xiv |
| Toward the Development of “Magmatology” | |
| <i>Ikuo Kushiro</i> | 1 |
| Nature and Climate Effects of Individual Tropospheric Aerosol | |
| Particles | |
| <i>Mihály Pósfai and Peter R. Buseck</i> | 17 |
| The Hellenic Subduction System: High-Pressure Metamorphism, Exhumation, Normal Faulting, and Large-Scale Extension | |
| <i>Uwe Ring, Johannes Glodny, Thomas Will, and Stuart Thomson</i> | 45 |
| Orographic Controls on Climate and Paleoclimate of Asia: Thermal and Mechanical Roles for the Tibetan Plateau | |
| <i>Peter Molnar, William R. Boos, and David S. Battisti</i> | 77 |
| Lessons Learned from the 2004 Sumatra-Andaman Megathrust Rupture | |
| <i>Peter Shearer and Roland Bürgmann</i> | 103 |
| Oceanic Island Basalts and Mantle Plumes: The Geochemical Perspective | |
| <i>William M. White</i> | 133 |
| Isoscapes: Spatial Pattern in Isotopic Biogeochemistry | |
| <i>Gabriel J. Bowen</i> | 161 |
| The Origin(s) of Whales | |
| <i>Mark D. Uhen</i> | 189 |
| Frictional Melting Processes in Planetary Materials: From Hypervelocity Impact to Earthquakes | |
| <i>John G. Spray</i> | 221 |
| The Late Devonian Gogo Formation Lagerstätte of Western Australia: Exceptional Early Vertebrate Preservation and Diversity | |
| <i>John A. Long and Kate Trinajstić</i> | 255 |

| | |
|---|-----|
| Booming Sand Dunes <i>Melany L. Hunt and Nathalie M. Vriend</i> | 281 |
| The Formation of Martian River Valleys by Impacts <i>Owen B. Toon, Teresa Segura, and Kevin Zahnle</i> | 303 |
| The Miocene-to-Present Kinematic Evolution of the Eastern Mediterranean and Middle East and Its Implications for Dynamics <i>Xavier Le Pichon and Corné Kreemer</i> | 323 |
| Oblique, High-Angle, Listric-Reverse Faulting and Associated Development of Strain: The Wenchuan Earthquake of May 12, 2008, Sichuan, China <i>Pei-Zhen Zhang, Xue-ze Wen, Zheng-Kang Shen, and Jiu-hui Chen</i> | 353 |
| Composition, Structure, Dynamics, and Evolution of Saturn's Rings <i>Larry W. Esposito</i> | 383 |
| Late Neogene Erosion of the Alps: A Climate Driver? <i>Sean D. Willett</i> | 411 |
| Length and Timescales of Rift Faulting and Magma Intrusion: The Afar Rifting Cycle from 2005 to Present <i>Cynthia Ebinger, Atalay Ayele, Derek Keir, Julie Rowland, Gezahegn Yirgu, Tim Wright, Manablob Belachew, and Ian Hamling</i> | 439 |
| Glacial Earthquakes in Greenland and Antarctica <i>Meredith Nettles and Göran Ekström</i> | 467 |
| Forming Planetesimals in Solar and Extrasolar Nebulae <i>E. Chiang and A.N. Youdin</i> | 493 |
| Placoderms (Armored Fish): Dominant Vertebrates of the Devonian Period <i>Gavin C. Young</i> | 523 |
| The Lithosphere-Asthenosphere Boundary <i>Karen M. Fischer, Heather A. Ford, David L. Abt, and Catherine A. Rychert</i> | 551 |

Indexes

| | |
|---|-----|
| Cumulative Index of Contributing Authors, Volumes 28–38 | 577 |
| Cumulative Index of Chapter Titles, Volumes 28–38 | 581 |

Errata

An online log of corrections to *Annual Review of Earth and Planetary Sciences* articles may be found at <http://earth.annualreviews.org>